

A QUANTITATIVE CYTOARCHITECTONIC  
ANALYSIS OF THE INTERPEDUNCULAR  
COMPLEX OF THE ALBINO RAT

Thesis for the Degree of M. A.  
MICHIGAN STATE UNIVERSITY

William Robert Ives

1968

## ABSTRACT

### A QUANTITATIVE CYTOARCHITECTONIC ANALYSIS OF THE INTERPEDUNCULAR COMPLEX OF THE ALBINO RAT

By

William Robert Ives

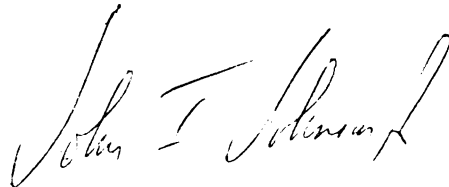
The interpeduncular complex (IPN), situated on the medio-ventral surface of the midbrain, is universally present in all vertebrates including man. Experiments on the functional significance of this structure, thus far unproductive, have generally assumed cytoarchitectonic homogeneity although this is contradicted by a number of qualitative studies. Because of the lack of quantitative data on the structure of the IPN the present study has undertaken an analysis of this structure using measures of cell size and packing density as measures of subnuclear differentiation. Cell size (area) and density were measured in 4 spatially separate cell groups; pars lateralis (PL), pars medialis (PM), pars dorsalis parvocellularis (PDP), and pars dorsalis magnocellularis (PDM). The IPN of 3 normal, Nissl-stained, albino rats, sectioned in the horizontal, sagittal, and coronal planes of section served as material. 60 cells were randomly sampled from each of the 4 subnuclei for each of the 3 planes of section and their areas determined by planimetry. Density was measured within each subnucleus by counting the numbers of cells contained in several sample volumes of tissue. PDM had the largest cell size and the lowest density of any of the 4 subnuclei while PDP had the smallest cell size and the highest density. PL and PM were intermediate in





William Robert Ives

both cell size and packing density and were not significantly different from one another. The differences were tested by a 2 way analysis of variance and Newman-Keuls tests at the .01 level of confidence. The absence of any quantitative differences between PL and PM casts doubt upon earlier distinctions based on qualitative studies of these 2 subnuclei. The distinction between PL and PM is a spatial one and not cytoarchitectural while PDM and PDP present both spatial and cytoarchitectural differences. These quantitative differences in cytoarchitecture may imply functional differentiation within the IPN which may help to explain the variety of behavioral deficits observed after gross lesions of this structure.

A handwritten signature in cursive script, appearing to read "John I. Johnson". The signature is written in dark ink and is positioned below the main body of text.

A QUANTITATIVE CYTOARCHITECTONIC ANALYSIS  
OF THE INTERPEDUNCULAR COMPLEX  
OF THE ALBINO RAT

By

WILLIAM ROBERT IVES

A THESIS

Submitted to  
Michigan State University  
in partial fulfillment of the requirements  
for the degree of

MASTER OF ARTS

Department of Psychology

1968



60307  
1000

## ACKNOWLEDGEMENTS

The author wishes to express his gratitude to the following professors whose guidance during my education has been invaluable; Dr. G. I. Hatton who first aroused my interest in the nervous system, Dr. T. W. Jenkins who provided me with an invaluable introduction to neuroanatomy, Dr. J. I. Johnson who furthered my interest in the nervous system, and Dr. M. Balaban who introduced me to developmental neuroanatomy.

To my wife, whose efforts in reaching this stage in my education have been far greater than mine, I dedicate this thesis.

This research has been supported by research grant NB 05982 to Dr. J. I. Johnson and NIH training grant MH 10611.

## TABLE OF CONTENTS

	page
ACKNOWLEDGEMENTS.....	ii
LIST OF TABLES.....	iv
LIST OF FIGURES.....	v
ABBREVIATIONS USED IN PLATES 1-6.....	vi
INTRODUCTION.....	1
METHOD.....	8
RESULTS.....	10
DISCUSSION.....	23
REFERENCES.....	31
PLATES.....	33
APPENDIX A.....	39

# LIST OF TABLES

Table		Page
1.	Summary of the results of the analysis of variance conducted on the cell size data.....	12
2.	Summary of the results of the Newman-Keuls tests conducted on the cell size data.....	12
3.	Cell size ratios computed as the ratio between a given subnucleus and PM.....	12
4.	Summary of the analysis of variance conducted on the density results.....	19
5.	Summary of the results of the Newman-Keuls tests.....	19
6.	Density ratios computed as the ratio between a given subnucleus and PM.....	19



# LIST OF FIGURES

Figure	page
1. A schematic representation of the generalized fiber connections of the vertebrate IPN.....	3
2. A schematic representation of the subnuclei of the cat IPN after Berman and Bowers (1967)....	5
3. A schematic representation of the subnuclei of the rat IPN.....	7
4. Results of cell area measurements for PM.....	13
5. Results of cell area measurements for PL.....	14
6. Results of cell area measurements for PDP.....	15
7. Results of cell area measurements for PDM.....	16
8. Composite of the histograms of Figures 4-7 for purposes of comparison.....	17
9. Results of density measurements for PL and PM.....	20
10. Results of density measurements for PDM and and PDP.....	21
11. Composite of the histograms of Figures 9 and 10 for purposes of comparison.....	22

Plate	page
1. Caudal section through the midbrain at the level of the decussation of the superior cerebellar peduncle (DBC).....	33
2. Caudal section through the midbrain at the level of the trochlear nucleus (IV).....	34
3. Coronal section through the midbrain at the level of the caudal extent of the superior colliculus (COL. SUP.).....	35
4. Coronal section through the midbrain at the level of the oculomotor nucleus (III).....	36
5. Coronal section through the midbrain at the level of the red nucleus (N. RUB.).....	37
6. Coronal section through the midbrain at rostral levels through the IPN.....	38

# ABBREVIATIONS USED IN PLATES 1-6

CIC.....	commissure of the inferior colliculus
COL. SUP. ....	superior colliculus
COR. PIN. ....	pineal body
DBC.....	decussation of the superior cerebellar peduncle
DEC. TEG. DORS. ....	dorsal tegmental decussation
DEC. TEG. VENT. ....	ventral tegmental decussation
FLM.....	medial longitudinal fasciculus
GR. CENT. ....	central gray
GR. PONT. ....	pontine gray
LEM. MED. ....	medial lemniscus
N. INTERPED. PARS DORSALIS PARS MAGNO.....	interpeduncular nucleus pars dorsalis pars magnocellularis
N. INTERPED. PARS DORSALIS PARS PARVO. ....	interpeduncular nucleus pars dorsalis pars parvocellularis
N. INTERPED. PARS LATERALIS.....	interpeduncular nucleus pars lateralis
N. INTERPED. PARS MED. ....	interpeduncular nucleus pars medialis
N. LIN. ....	linear nucleus
N. OCULO. ....	oculomotor nucleus (III)

ABBREVIATIONS USED IN PLATES 1-6  
(continued)

N. RUB. ....	red nucleus
N. TROCH. ....	trochlear nucleus (IV)
PED. CER. ....	cerebral peduncle
PED. MAM. ....	mammillary peduncle
RAD. MEY. ....	radiations of Meynert
SUB. NIG. ....	substantia nigra
TR. CORT. SP. ....	corticospinal tract
TR. HAB. PED. ....	habenulopeduncular tract
III.....	oculomotor nerve



## INTRODUCTION

### General Anatomy

Because of the juxtaposition of the interpeduncular nucleus (IPN) and the posterior perforated substance Forel (1877) first termed this nucleus das Ganglion der lamina perforata posterior. Gudden (1881) later termed this cell group das Ganglion interpedunculare because of its position between the cerebral peduncles in mammals. Subdivisions of the nucleus were not described by these early investigators although Cajal (1952) described a stratification of the nucleus into two layers in the rabbit. The outer layer (i.e. dorsal) consisted of large multipolar cells (peripheral zone) while the inner (i.e. ventral) layer was described as consisting of small to medium sized cells (plexiform layer). These early descriptions for mammals were accepted until the work of Huber, Crosby, Woodburne, Gillian, Brown, and Tamthai (1943) in which it was noted that the IPN of a number of mammals (mink, rabbit, cat, dog, sheep, pig, rat, and armadillo) appeared to consist of two spatially and cytoarchitectonically distinct subnuclei; a large celled lateral subnucleus and a smaller celled medial subnucleus. According to the latter authors the IPN reached its greatest development in the rabbit where it consisted of three

subnuclei; a compact dorsal portion, a large celled lateral portion, and a small celled medial portion.

Work on the submammalian IPN has been done by Herrick (1917) in the mudpuppy, Necturus, and by Jansen (1930) in the hagfish, Myxine. In the hagfish the nucleus consists of a rostrally located mesencephalic division which consists of large multipolar cells and a caudally located rhombencephalic division which contains large and small spindle shaped cells. A similar subdivision of the nucleus into rostral and caudal components has been described for Necturus.

A schematic drawing of the generalized fiber connections of the vertebrate IPN is shown in Figure 1. The connections are general in the sense that all vertebrates minimally have them. The IPN receives a large contingent of fibers from the habenulae as the habenulopeduncular tract (HPT) which contains fibers from both the lateral and medial habenular nuclei (Kappers, Huber, and Crosby, 1936). The IPN is also afferently connected with the mammillary bodies via the mammillopeduncular tract. The efferent outflow of the nucleus is directed to the dorsal tegmental nucleus of the central gray via the pedunculotegmental tract. The dorsal tegmental nucleus contributes its fibers to the dorsal longitudinal fasciculus which synapses with several visceral efferent cranial nerve nuclei (VII, IX, X, XI) (Zeman and Innes, 1963).

Several general features of the vertebrate IPN need to be noted. That the nucleus is divided into at least two subnuclei in many vertebrates is quite evident. In Myxine and Necturus

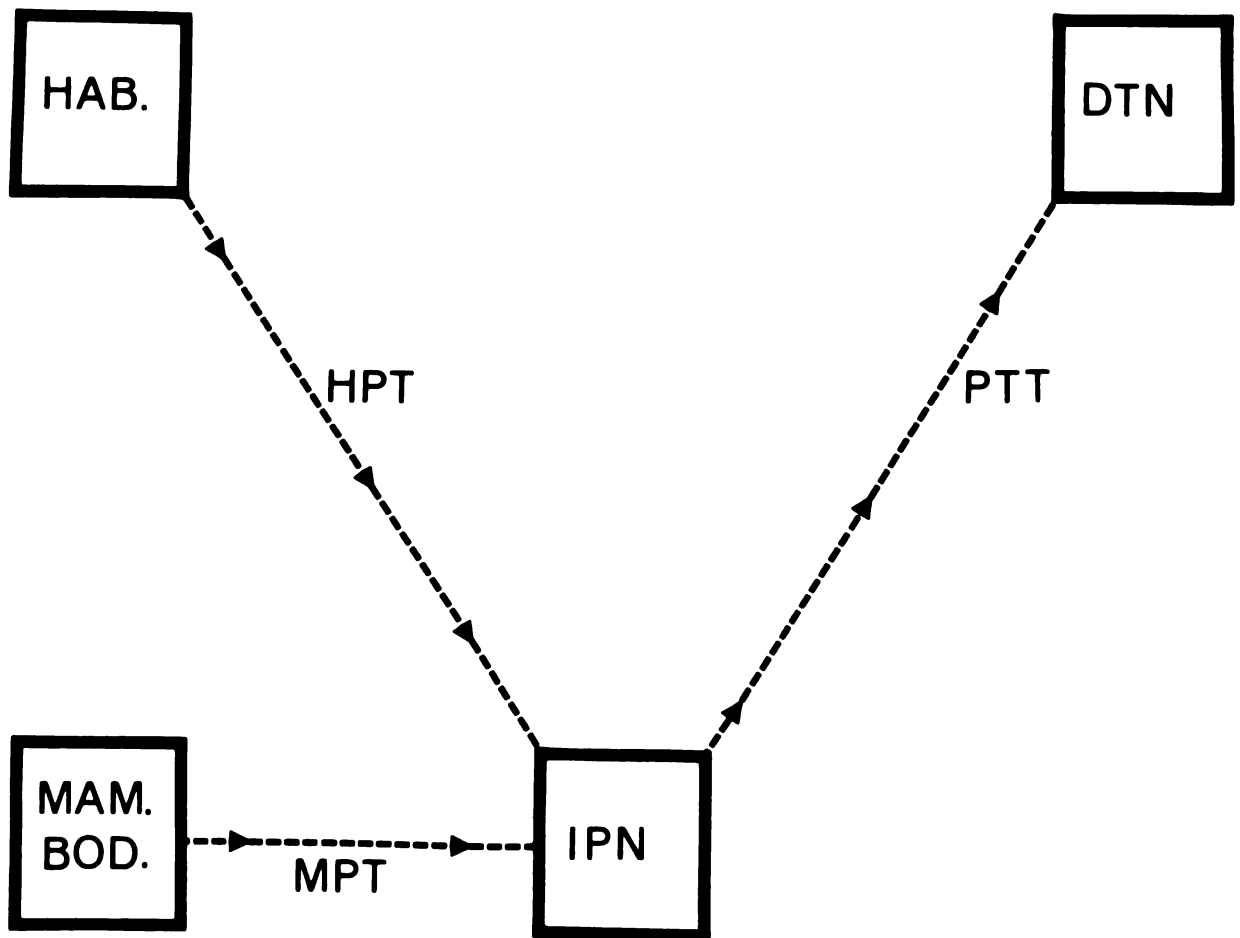


Figure 1. A schematic representation of the generalized fiber connections of the vertebrate IPN. Arrows indicate the direction of conduction of nerve impulses. HAB.= habenula, DTN= dorsal tegmental nucleus, MAM. BOD.= mammillary body, IPN= interpeduncular nucleus, HPT= habenulopeduncular tract, PTT= pedunculotegmental tract, MPT= mammillopeduncular tract.



these divisions are rostral and caudal and as we ascend the phyletic scale they become medial and lateral. This shift in position of the subnuclei follows the shift in the position of the habenular subnuclei from a rostral-caudal subdivision to a medial-lateral one. The HPT also has been described as consisting of contributions from both the habenular subnuclei (Kappers, Huber, and Crosby, 1936).

The general existence of a divided input (HPT) to a nucleus that also exhibits divisions indicates that there may be a certain specificity of projection upon the IPN. A given habenular subnucleus might project to a given IPN subnucleus. One might also hypothesize that there exists some specificity of output through the pedunculotegmental tract although there is no experimental evidence to corroborate either of these points.

### The Problem

A recent study by Berman and Bowers (1967) has renewed interest in the cytoarchitectonics of the IPN. They described five subnuclei of the cat IPN which differ from one another on the basis of cell size, staining characteristics, and packing density. These subnuclei are the posterior, apical, central, paramedian, and intrafascicular (see Figure 2).

"The posterior nucleus comprises an outer division which forms a cellular cup surrounding the caudal part of the complex, and a bifurcated inner division separated from the outer by a cell sparse zone. The apical nucleus is embedded in the dorsal aspect of the outer division. The paramedian nuclei are paired columns of cells on either side of, but clearly separated from the inner division of the posterior nucleus. The central nucleus is an elongated structure rostral to, and partly fused with the inner

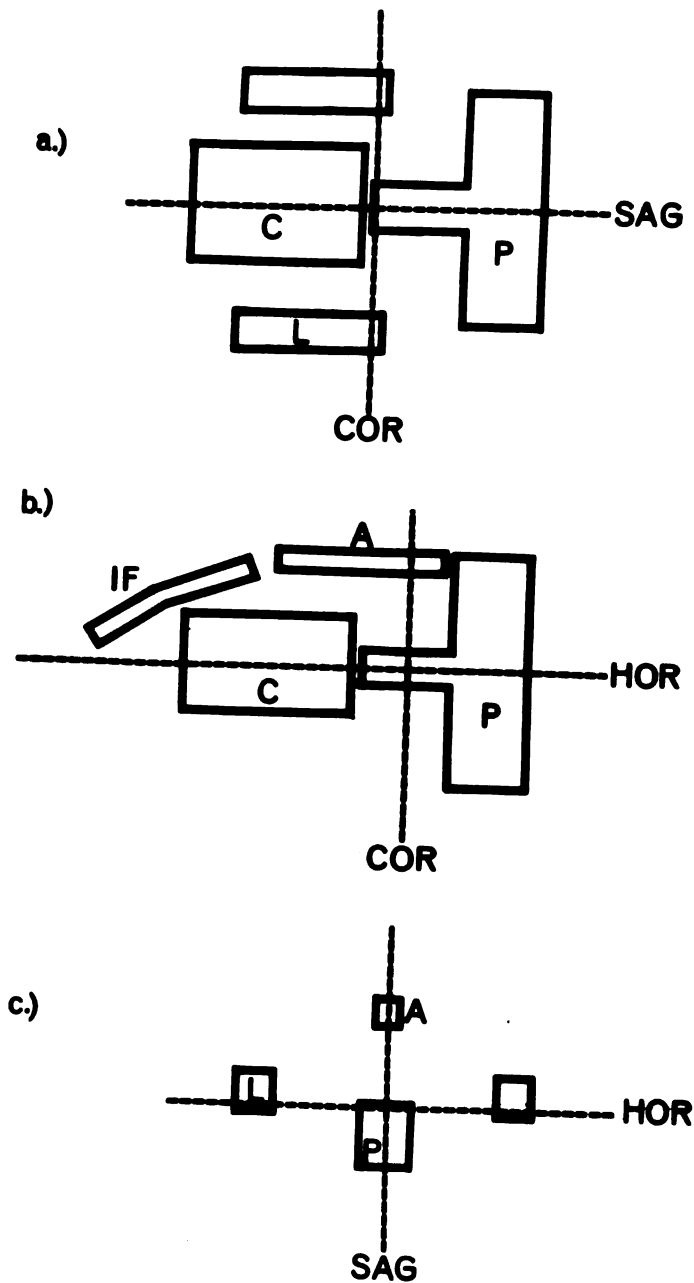


Figure 2. A schematic representation of the subnuclei of the cat IFN after Berman and Bowers (1967). In a, b, and c the nucleus is shown in the horizontal, sagittal, and coronal planes of section, respectively. A= apical, C= central, F= posterior, L= paramedian, and IF= intrafascicular.

division of the posterior nucleus. At the rostral end of the complex a fifth structure, the intrafascicular nucleus, forms a cap over the central nucleus, but extends beyond it as a narrow wedge in the median raphe between the two habenulopeduncular tracts." Berman and Bowers, 1967, p.213.

These authors stated that it was not possible to tell whether the intrafascicular nucleus was a part of the complex or a part of the central linear nucleus with which it merged.

My own work in the rat (see plates and Figure 3) has indicated the presence of four subnuclei which differ from one another on the basis of location and/or cell size. These are the pars dorsalis magnocellularis (PDM), pars dorsalis parvocellularis (PDP), pars lateralis, and pars medialis. PDM consists of large cells which lie in the dorsocaudal third of the complex. PDP, located immediately rostral to PDM, consists of small spherical cells with lightly staining nucleoli. In sections through the red nucleus PDP turns ventral and comes to occupy the medial portion of the nucleus as well. PL consists of two well defined groups of cells which lie at the lateral extremities of the nucleus. PM is located just ventral to PDM and PDP and medial to PL. It is separated from all the above subnuclei by areas of lower cell density.

The purpose of the present study was to quantitatively assess the nature of the aforementioned IPN subnuclei through measurement of cell size and packing density within the subnuclei. The values obtained for each of these measures was then compared with similar measurements for the other subnuclei through the use of appropriate statistical tests.

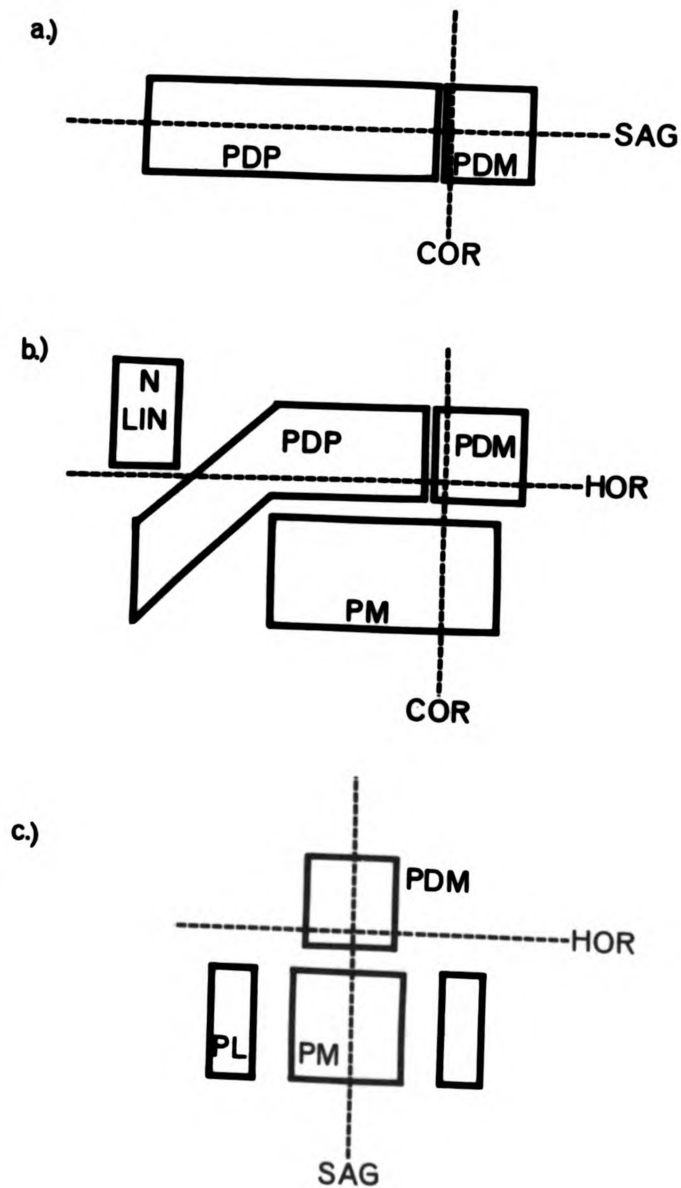


Figure 3. A schematic representation of the subnuclei of the rat IPN. In a, b, and c the nucleus is shown in the horizontal, sagittal, and coronal planes of section, respectively. PL= pars lateralis, PM= pars medialis, PDP= pars dorsalis parvocellularis, PDM= pars dorsalis magnocellularis, and N LIN= linear nucleus.

## METHOD

### Specimens

Three albino rats were perfused intracardially with .87% saline solution followed by a .87%-10% formalin mixture and their brains removed and photographed. The brains were embedded in celloidin and sectioned a 25 microns in three planes of section, horizontal, coronal, and sagittal. Alternate sections were stained with iron hematoxylin for fibers (Sanides Haldenhain method) and thionin for cells bodies (Nissl method). Refer to appendix A for the details of the histological procedure.

### Cell Size Measurements

Cells of the four subnuclei were magnified 2800 times via a camera lucida attachment on a Zeiss microscope. Ten cells were randomly sampled from each subnucleus for six sections through the nucleus such that a total of 60 cells were sampled from each subnucleus for each plane of section. Only cells whose nucleoli were visible were sampled. The areas of the cells were determined by planimetry with a Keuffel and Esser compensating polar planimeter. Three area measurements were taken for each cell and the mean of these measurements used as an estimate of the true area.

### Packing Density Measurements

Densities were measured by counting the number of cells contained in a grid placed over the nucleus. The grid was a Whipple-Hauser disc which was placed directly in the ocular of the microscope. Knowing the thickness of the section and the area of the grid, volume could be determined by multiplying thickness times area. Dividing the number of cells in a sample volume by the sample volume gives the density of cells within a given subnucleus.

Thickness of a given section was measured in the following manner. The slide was placed on the microscope stage and the fine focus dial adjusted until the first cell came into focus. At this point the number on the focus vernier was read. The fine focus knob was then turned until the thickness of the section had been focused through and the last cell was in focus. The vernier was then read again and one reading subtracted from the other. The resulting number was the thickness of the section in microns. Thickness was measured three times for a given section and the mean of the measurements used as an estimate of the true thickness of the section. In order to avoid errors due to differential thickness within a given section measurements were only conducted upon the IPN and on no other portion of the section.

## RESULTS

### Descriptive Anatomy

Plates 1-6 show the nuclear configuration of the IPN and surrounding midbrain structures in a caudal to rostral sequence. In caudal sections through the midbrain (Plates 1&2) the IPN shows a division into three subnuclei, pars lateralis (PL), pars medialis (PM), and pars dorsalis magnocellularis (PDM). PL and PM are particularly well developed at this level in terms of size and in fiber preparations fibers can be seen issuing from the lateral borders of PM. The cells of PDM, while being sharply segregated from the rest of the nucleus, appear to trail off into the overlying nucleus centralis superior.

In middle and rostral sections through the midbrain (Plates 3-6), PDM can be seen to be replaced by pars dorsalis parvocellularis (PDP) on the dorsal aspect of the nucleus. In the most rostral sections (Plates 5&6) PDP turns ventral to replace PL and PM.

### Cell Size

The results of the cell area measurements are presented in Figures 4-8. On the abscissa of each figure is plotted the value for cellular area in microns<sup>2</sup> X 10, while the ordinate plots the frequency of occurrence of a given cell size. A two-way analysis of variance revealed a significant difference in mean cell areas between the three planes of section ( $F=33.33$ ,

2/708 df,  $p < .01$ ), a significant difference in mean cell areas between divisions ( $F=236.80$ , 3/708 df,  $p < .01$ ) and a significant interaction ( $F=4.25$ , 6/708 df,  $p < .01$ ). The results of this analysis are presented in tabular form in table 1.  $\omega^2$  (decimal fraction of the variance accounted for by the treatments) for planes was .04, for divisions .46, and for the interaction .01. Comparisons between all pairs of means by the method of Newman and Keuls (Table 2) revealed that the mean cell sizes within all subnuclei were significantly different from one another with five exceptions: PDPsag=PDPcor, PDPsag=PDPphor, PMcor=PLcor, PMSag=PLsag, PMhor=PLhor.

In order to ascertain whether or not the differences in cell size between planes (within a given subnucleus) could be attributed to shrinkage differences or differences in the actual orientation of the cells, ratios were computed. Three ratios for each plane were computed, PL/PM, PDM/PM, and PDP/PM. The values for these ratios are presented in table 3. It can easily be seen that the ratios remain essentially constant across planes which at least strengthens the argument for the cause of the differences being shrinkage. No statistical tests were conducted on these data.

### Density

The results of the density measurements are presented in figures 9-11. The abscissa of each histogram plots the density as cells/micron<sup>3</sup>  $\times 10^{-4}$  and the ordinate plots the frequency of occurrence of a given density. A two-way analysis



Table 1. Summary of the results of the analysis of variance conducted on the cell size data. \* =  $p < .01$

<u>SOURCE</u>	<u>SUM OF SQUARES</u>	<u>df</u>	<u>MEAN SQUARE</u>	<u>F</u>	<u><math>\omega^2</math></u>
Planes of section	282.69	2	141.34	33.33*	.04
Subnuclei	3,012.17	3	1,004.05	236.80*	.46
Interaction	120.07	6	20.01	4.71*	.01
Error	3,011.63	708	4.25	-----	---
Total	6,426.56	719	-----	-----	---

Table 2. Summary of the results of the Newman-Keuls tests conducted on the cell size data. Lines beneath two subnuclei indicate that they are not different from one another at the .01 level of confidence.

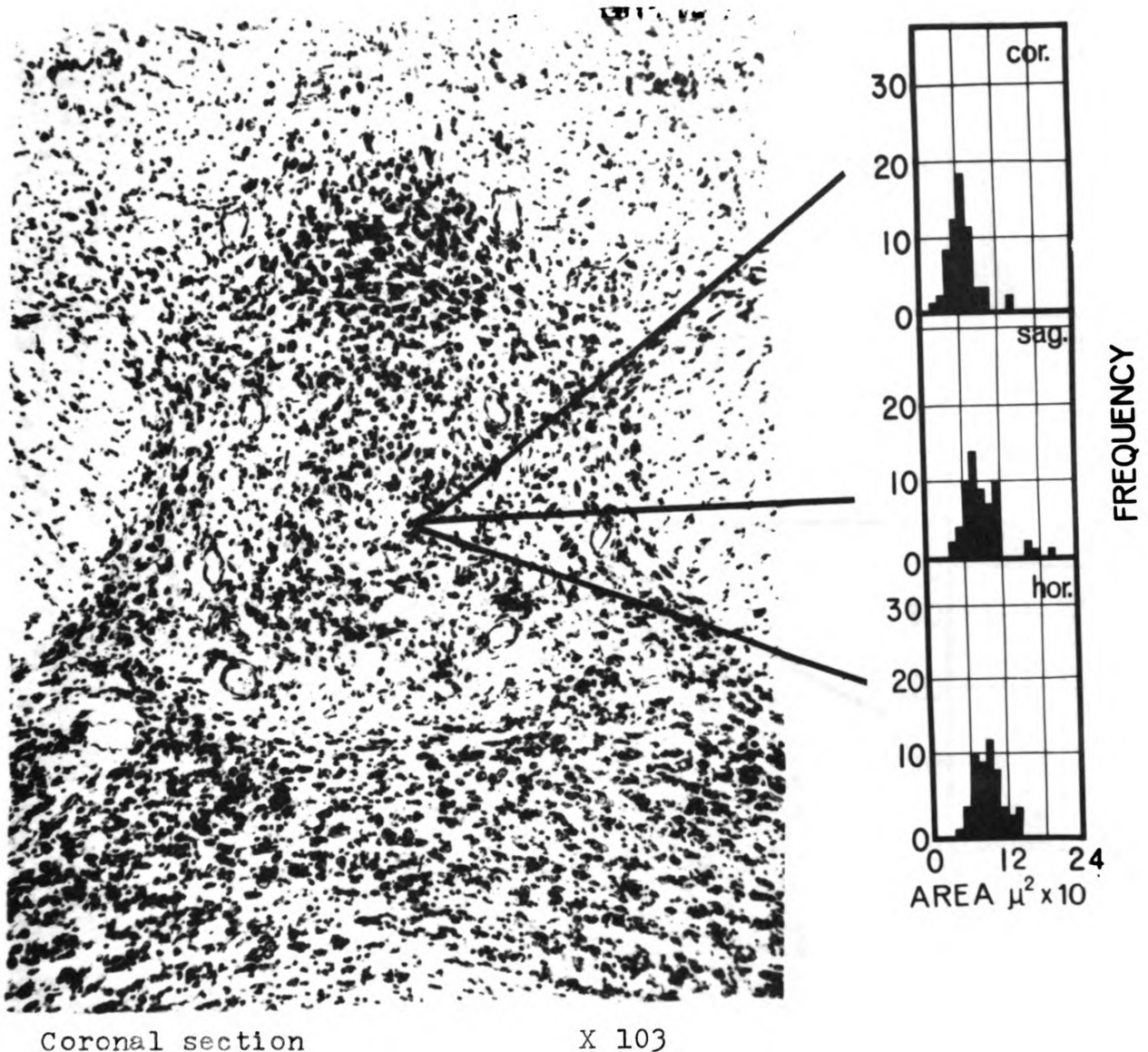
PDP<sub>c</sub> PDP<sub>s</sub> PDP<sub>h</sub> PM<sub>c</sub> PL<sub>c</sub> PM<sub>s</sub> PM<sub>h</sub> PL<sub>s</sub> PL<sub>h</sub> PDM<sub>c</sub> PDM<sub>s</sub> PDM<sub>h</sub>

_____											
	_____										
		_____									
			_____								
				_____							
					_____						
						_____					
							_____				
								_____			

\*\*\*\*\*

Table 3. Cell size ratios computed as the ratio between a given subnucleus and PM.

<u>CORONAL</u>	<u>SAGITTAL</u>	<u>HORIZONTAL</u>
PL/PM=1.00	PL/PM=1.09	PL/PM=1.05
PDM/PM=1.63	PDM/PM=1.34	PDM/PM=1.44
PDP/PM=.53	PDP/PM=.52	PDP/PM=.57



Coronal section

X 103

Figure 4. Results of cell area measurements for PM. In this and the following figures the results are based on a random sample of 60 cells from each of the three planes of section. The means and standard deviations for the respective planes are  $69 \text{ microns}^2 \pm 20$  for the coronal plane,  $85 \text{ microns}^2 \pm 24$  for the sagittal plane, and  $89 \text{ microns}^2 \pm 25$  for the horizontal plane. Comparisons of the means by the Newman-Keuls method revealed  $PM_c \neq PM_s$  and  $PM_s \neq PM_h$  at the .01 level of confidence. The section is approximately at the level of plate 2.

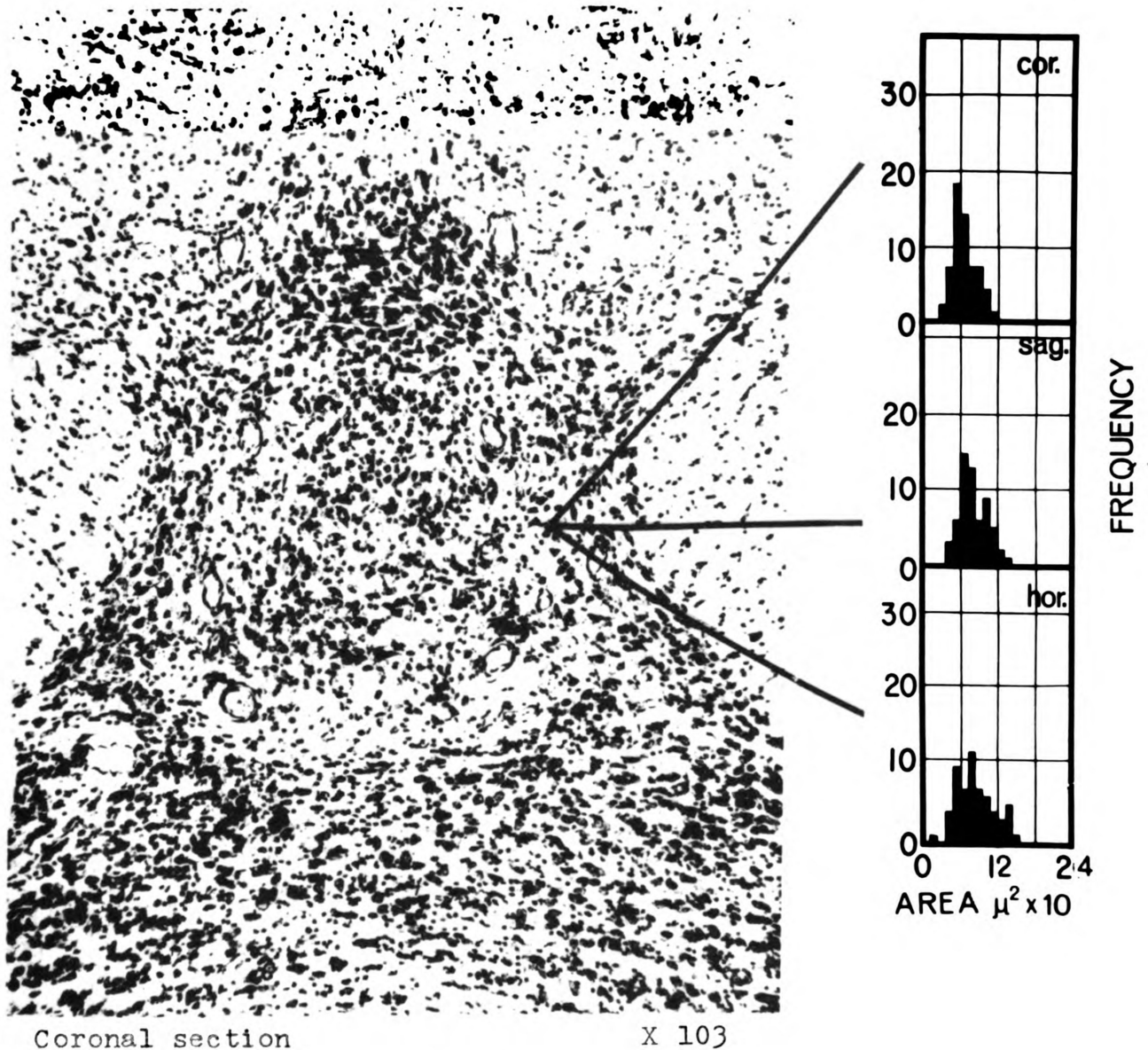


Figure 5. Results of cell area measurements for PL. The means and standard deviations for the respective planes of section are  $69 \text{ microns}^2 \pm 22$  for the coronal plane,  $93 \text{ microns}^2 \pm 29$  for the sagittal plane, and  $94 \text{ microns}^2 \pm 26$  for the horizontal plane. Comparisons between the means by the Newman-Keuls method revealed  $PL \neq PL_h$ ,  $PL \neq PL_s$ , and  $PL = PL_h$  at the .01 level of confidence. The section is approximately at the level of Plate 2.

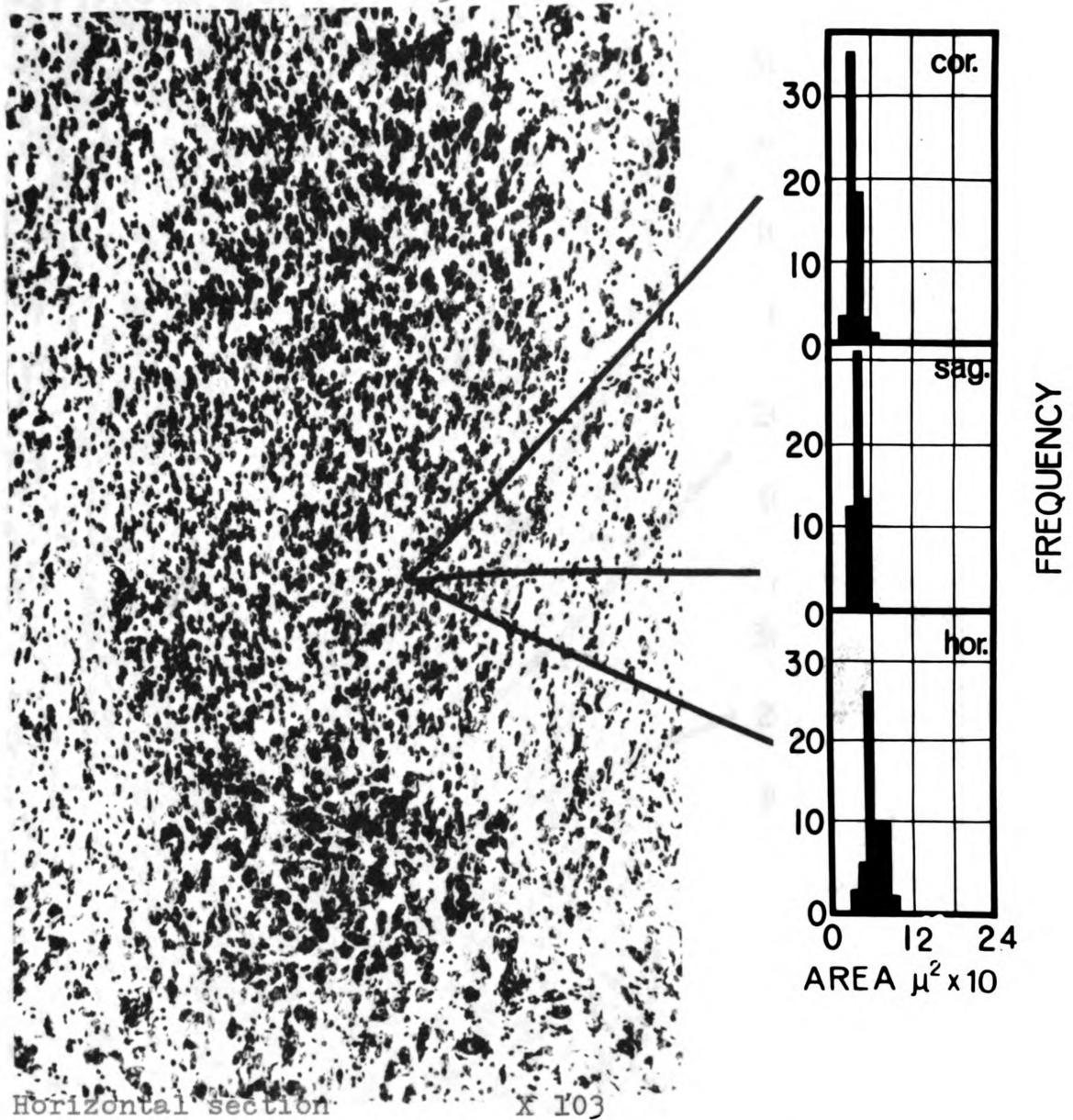


Figure 6. Results of cell area measurements for PDP. The means and standard deviations for the respective planes of section are  $36 \text{ microns}^2 \pm 8$  for the coronal plane,  $45 \text{ microns}^2 \pm 9$  for the sagittal plane, and  $51 \text{ microns}^2 \pm 14$  for the horizontal plane. Comparisons between the means by the Newman-Keuls method revealed  $PDP_c \neq PDP_h$  at the .01 level of confidence.

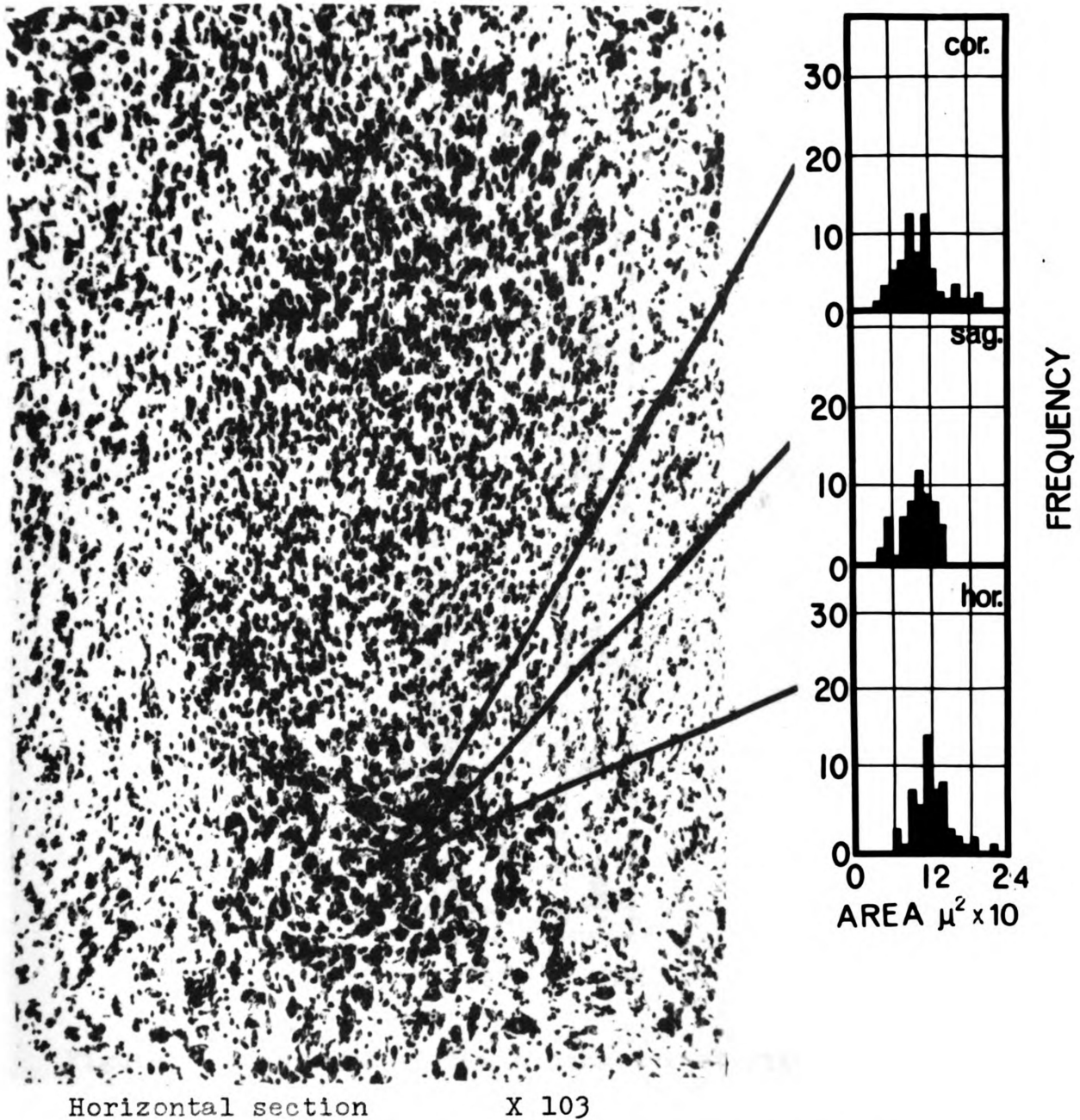


Figure 7. Results of cell area measurements for PDM. The means and standard deviations for the respective planes are  $112 \text{ microns}^2 \pm 36$  for the coronal plane,  $113 \text{ microns}^2 \pm 33$  for the sagittal plane, and  $129 \text{ microns}^2 \pm 36$  for the horizontal plane. Comparisons between the means by the Newman-Keuls method revealed  $PDM_c \neq PDM_h$  at the .01 level of confidence.

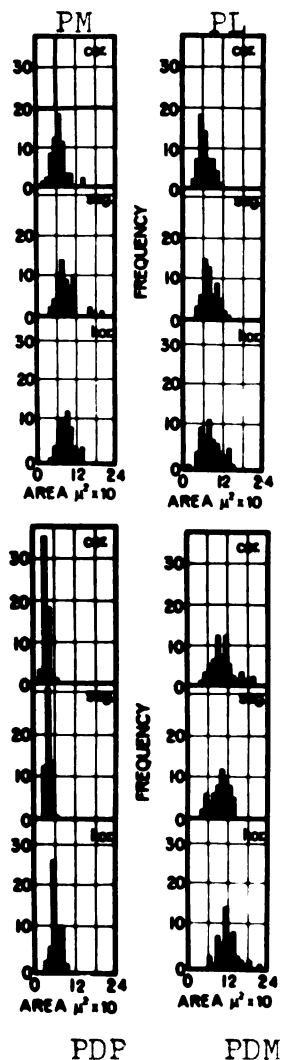


Figure 8. Composite of the histograms of Figures 4-7 for purposes of comparison. Within planes comparisons of the means by the Newman-Keuls method revealed the following:  
Coronal plane: PL=PM. PDP and PDM were different from one another and PL and PM at the .01 level of confidence;  
Sagittal plane: PL=PM. PDP and PDM were different from one another and PL and PM at the .01 level of confidence;  
Horizontal plane: PL=PM. PDP and PDM were different from one another and PL and PM at the .01 level of confidence.



of variance (table 4) revealed a significant difference in the mean cell densities between planes ( $F=2.495$ ,  $2/60$  df,  $p < .05$ ) and a significant difference between subnuclei ( $F=32.988$ ,  $3/60$  df,  $p < .01$ ). There was no significant interaction.

All possible comparisons of the means by the method of Newman and Keuls (Table 5) revealed  $PM=PL$  within each of the three planes of section while PDP was significantly more dense than PDM for the three planes of section.

As with cell size, ratios were computed to ascertain what the differences in density between planes (within divisions) indicated. These ratios, computed as the ratio of a given subnucleus to PM are shown in Table 6. The results present a picture of equality across planes with two exceptions: both  $PDM/PM$  and  $PDP/PM$  in the horizontal plane of section are higher than the other corresponding ratios.

After the research was completed it was discovered that there was an error in determining section thickness by the method described previously. This error was due to the refractive index of the mounting medium. The data was recalculated under the assumption that the sections were uniformly cut at 25 microns. Although the mean densities changed in all cases after the recalculation the ratios between the subnuclei were not appreciably altered.

Table 4. Summary of the analysis of variance conducted on the density results.\*= significant at .01 level of confidence.

SOURCE	SUM OF SQUARES	df	MEAN SQUARE	F	$\omega^2$
Planes of section	14.81	2	7.40	2.49*	.01
Subnuclei	293.72	3	97.90	32.98*	.56
Interaction	16.49	6	2.74	.92	---
Error	178.09	60	2.96	-----	---
Total	503.11	71	-----	-----	---

Table 5. Summary of the results of the Newman-Keuls tests. A line beneath 2 subnuclei indicates that they are not significantly different at the .01 level of confidence.

$\text{PM}_c$	$\text{PM}_h$	$\text{PL}_c$	$\text{PM}_s$	$\text{PL}_h$	$\text{PL}_s$	$\text{PDM}_c$	$\text{PDM}_s$	$\text{PDM}_h$	$\text{PDP}_c$	$\text{PDP}_s$	$\text{PDP}_h$
_____											
_____											
_____											
	_____										
	_____										
	_____										
		_____									
		_____									
			_____								
			_____								
				_____							
				_____							
					_____						
					_____						
						_____					
							_____				
								_____			

Table 6. Density ratios computed as the ratio between a given subnucleus and PM

<u>CORONAL</u>	<u>SAGITTAL</u>	<u>HORIZONTAL</u>
PL/PM=1.11	PL/PM=1.07	PL/PM=1.06
PDM/PM=1.34	PDM/PM=1.24	PDM/PM=1.91
PDP/PM=3.70	PDP/PM=3.57	PDP/PM=5.26



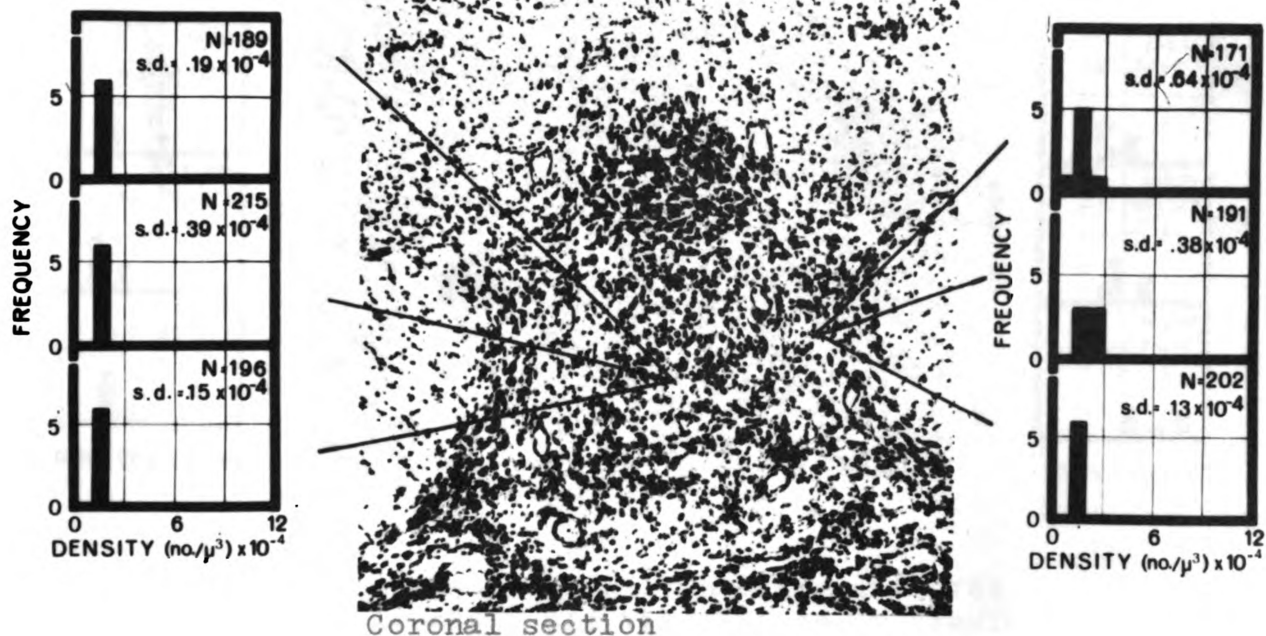


Figure 9. Results of density measurements for PL and PM. In this figure and Figures 10 and 11 the abscissa represents the density as cells/micron<sup>3</sup> X 10<sup>-4</sup> while the ordinate represents the frequency of occurrence of a given density. In the upper right hand corner of each histogram is the number of cells counted and the standard deviation of the sample. The coronal plane is represented by the upper histogram, the sagittal plane by the middle histogram, and the horizontal plane by the lower histogram. Mean densities for the respective planes were:

#### Coronal

PL	$1.638 \times 10^{-4}$	cells/micron <sup>3</sup>
PM	$1.469 \times 10^{-4}$	"

#### Sagittal

PL	$1.789 \times 10^{-4}$	"
PM	$1.663 \times 10^{-4}$	"

#### Horizontal

PL	$1.731 \times 10^{-4}$	"
PM	$1.622 \times 10^{-4}$	"

Within planes comparisons of the means by the Newman-Keuls method revealed no significant differences between PL and PM.

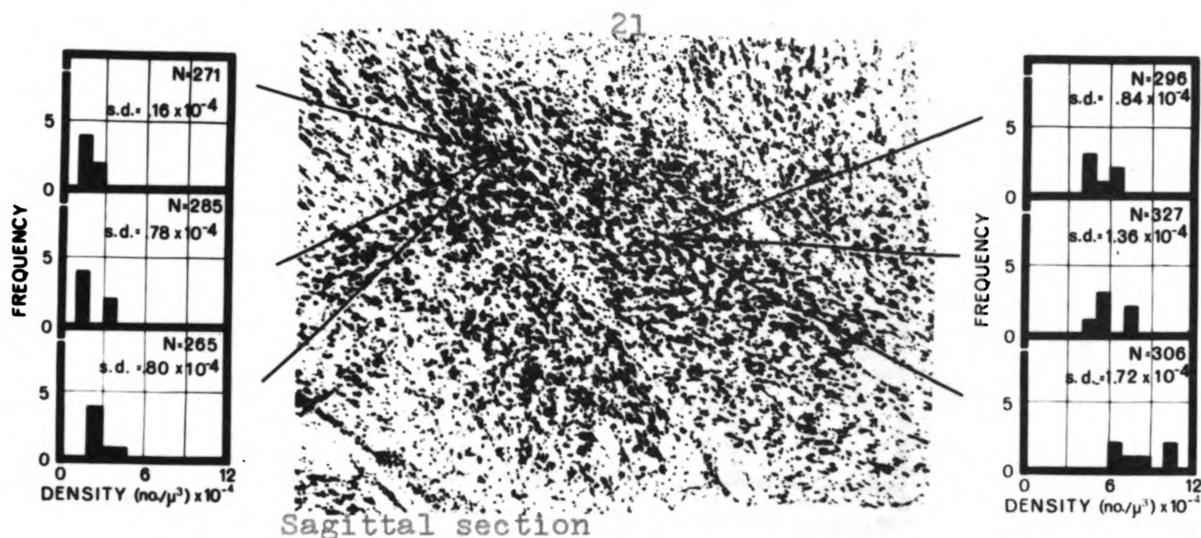


Figure 10. Results of density measurements for PDM and PDP. Ordinate and abscissa are the same as in Figure 9. In the upper right hand corner of each histogram is the number of cells counted and the standard deviation of the sample. The upper histogram represents the coronal plane, the middle histogram represents the sagittal plane, and the lower histogram represents the horizontal plane. The means for the respective planes were:

#### Coronal

PDP	$5.938 \times 10^{-4}$	cells/micron <sup>3</sup>
PDM	$1.979 \times 10^{-4}$	"

#### Sagittal

PDP	$5.935 \times 10^{-4}$	"
PDM	$2.072 \times 10^{-4}$	"

#### Horizontal

PDP	$8.171 \times 10^{-4}$	"
PDM	$3.148 \times 10^{-4}$	"

Within planes comparisons of the means by the Newman-Keuls method revealed PDP significantly greater in density than PDM at the .01 level of confidence.

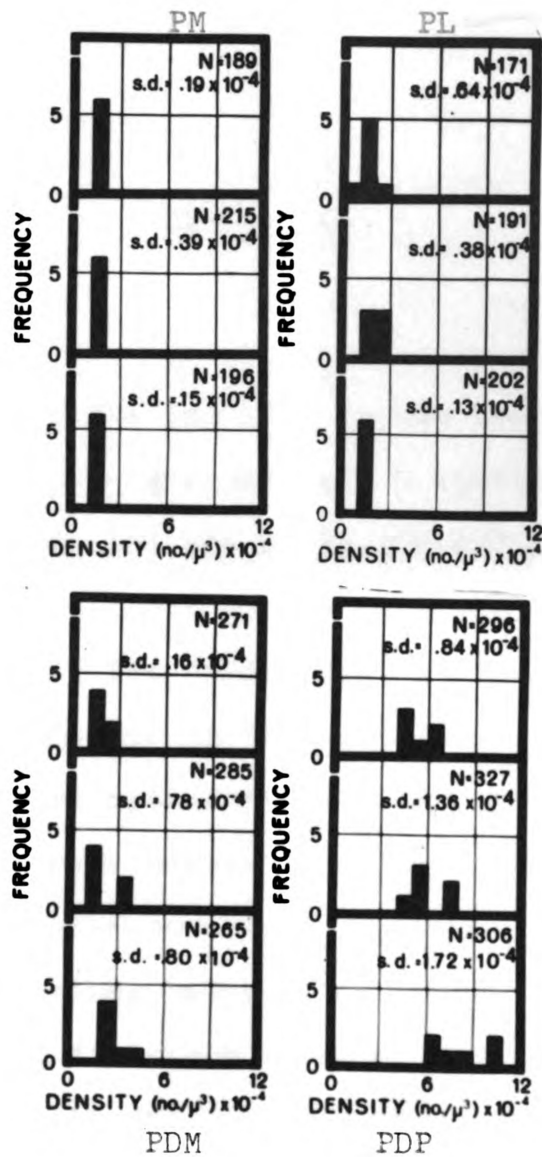


Figure 11. Composite of the histograms of Figures 9 and 10 for purposes of comparison. Refer to Table 5 for results of between planes comparisons of the mean cell densities.

## DISCUSSION

### An Overview

Generally, in the rat IPN, it has been found that the constituent cells are grouped into 4 spatially distinct subnuclei. These subnuclei are PL, PM, PDM, and PDP. While the latter two subnuclei exhibit marked differences in both cell size and packing density the former two are not significantly different from one another in terms of these measures. Because of the quantitative cytoarchitectonic similarity between PL and PM one might hypothesize that they are functionally similar subnuclei which have been separated from one another by two intrinsic fiber bands. That quantitatively different cytoarchitectonic divisions exist within the IPN is assumed to indicate a functional differentiation of the nucleus.

### Cell Size

The high value for  $\omega^2$  for subnuclei (.46) and its relatively low value for the interaction and planes effects indicates that a knowledge of the subnuclei is a more efficacious predictor of cell size than is a knowledge of planes of section or both subnuclei and planes of section. This measure may be interpreted as indicating that our uncertainty about the cell size is reduced by 46% if we know the division from which the cell was sampled. This is compared with a reduction

of uncertainty of only 4% if we know the plane in which the nucleus was sectioned. Given both planes of section and sub-nucleus the uncertainty in predicting cell size is only reduced by 1% over that given by the other two effects independently.

The virtual constancy of the ratios (Table 3) across planes (for a given ratio) indicates that differences which occurred between certain divisions across planes are probably due to shrinkage. Thus, for example, PLcor was significantly different from PLsag and PLhor, although the ratio, PL/PM, was essentially constant for the respective three planes. We can conclude that within animal comparisons (i.e. within a given plane of section) of mean cell size in different subnuclei can be done directly. This is opposed to between animal comparisons (between planes of section) which must take the form of ratios or some other similar technique which effectively cancels out the variance due to histological procedures.

The general results of the Newman-Keuls test indicate that within a given plane of section PL and PM do not differ significantly in their mean cell size. This is to say that the samples of cells from these two divisions are not different in terms of cell size although their spatial location is different. The predictive value of this result is obvious. Given a sample of cells whose mean is similar to that of PL or PM it would be impossible to determine, on the basis of cell size, whether or not the cells had been sampled from PL or PM.

Given only cell size it is impossible to specify PL or PM. These subnuclei must be specified by their spatial location. This is not true of PDM and PDP as indeed the names are meant to imply. The latter two distributions of cell size are markedly different. The distribution of PDP has a relatively small variance and a mean cell size of approximately 40 microns<sup>2</sup> whereas the variance of the PDM cell size distribution is relatively greater and mean cell area is approximately 105 microns<sup>2</sup>.

Density

As with the cell size data, the subnuclei factor of the analysis of variance demonstrated a high value for  $\omega^2$  (.56). In terms of the predictive value this indicates that a knowledge of the subnucleus (i.e. which subnucleus) reduces our uncertainty as to the packing density of the constituent cells by 56%. This is to be compared with the relatively low value for the planes factor (.01).

In general the ratios were constant with 2 exceptions; both PDM/PM and PDP/PM were much greater than expected. This indicates that PDP and PDM are more densely packed in the horizontal plane than in the other two planes of section with respective means of  $8.171 \times 10^{-4}$  and  $3.148 \times 10^{-4}$  cells/micron<sup>3</sup>. Measurements of density in another rat brain sectioned in the horizontal plane were conducted in order to ascertain whether or not this finding was reliable. The means for this animal were PDM=  $2.837 \times 10^{-4}$  and PDP=  $7.215 \times 10^{-4}$  cells/ micron<sup>3</sup>. The corresponding ratios were PDM/PM= 1.71 and PDP/PM=4.37. The close correspondence between the means and ratios for the

two animals sectioned in the horizontal plane indicate that PDM and PDP are reliably more dense in the horizontal plane as opposed to either the sagittal or coronal planes of section.

An explanation of this paradoxical finding might be that these dorsal subnuclei are laminated. The distance between the laminae would be less than the average thickness of the sections since there were no areas of relatively low density found interspersed with areas of relatively high density.

### Synthesis

Huber, et.al. (1943) have described the rat IPN as consisting of a large celled lateral subnucleus and a smaller celled medial subnucleus. The results of the present study place these latter findings in doubt since it was shown that the lateral and medial subnuclei did not differ on the basis of either cell size or packing density. That these results were reliable across three animals obviates any explanation of these results as due to insufficient sample size. Furthermore, the ratio, PL/PM, remained essentially constant across animals which indicates that any observed differences between PL and PM across animals were probably due to extraneous factors (most likely differential shrinkage).

Employing the quantitative techniques described in the present paper it is possible to specify or define the component subnuclei of the IPN in terms of three numbers; a cell size term, a density term, and a coordinate or positional term. In certain cases, as for example with PDP and PDM, it is

possible to adequately describe the given subnucleus using only the first two terms. With PL and PM, though, position must be specified if we are to distinguish between these two subnuclei.

The use of quantitative techniques is important because they provide for a greater degree of interobserver reliability than has generally been present in neuroanatomy. Given the appropriate measuring devices it would be expected that another observer would find the same results as presented in this paper. This does not assume that another observer would arrive at exactly the same numbers. What it does imply is that another observer would obtain the same results relative to the present ones. By computing ratios between the different subnuclei for both density and cell size, extraneous factors such as differing fixation and dehydration times are effectively cancelled out.

The raison d'etre of the nuclear subdivisions is not clear. It is my assumption that these differences in the cytoarchitectonics of the rat IPN indicate functional differences. The basis for this assumption is that one would expect cell size and packing density within the nucleus to be randomly distributed. When it is not, as with the IPN, functional differentiation is the first choice as an explanation of the findings. There are two lines of evidence which support this assumption; biochemical studies and studies of the fiber connections of the IPN.

Friede (1959) and Manocha and Bourne (1966) have



reported in the guinea pig and squirrel monkey, respectively, that there is differing activity of succinic dehydrogenase (SDA) and cytochrome oxidase (CO) within the IPN. In both species the ventral portion of the nucleus exhibits a high activity of these enzymes while the dorsal portion exhibits very low activity of SDA and CO. The differences in the activity of these enzymes is related to the degree of capillarization which in turn is related to the degree of metabolic activity (Sharrer, 1945). The metabolic rate might be related to spontaneous activity within the nucleus which would predict a high spontaneous firing rate for cells in the ventral portion of the complex as opposed to those in the dorsal portion.

The fiber connections of the IPN have not been well studied in relation to the subnuclei described in the present paper. In the normal rat brains the author has observed that the fibers of the pedunculotegmental tract appear to issue from the lateral borders of PM. In the cat Smaha (1968) has provided some evidence that there are at least two efferent fiber systems of the IPN. One projects rostrally to the intralaminar system of the dorsal thalamus and the thalamic reticular nucleus. The caudally projecting fibers travel to the ventral tegmental nucleus of Gudden and the inferior olive. It is unfortunate that these fiber projections were not correlated with the nuclear morphology elucidated by Berman and Bowers (1967).

Afferently, the HPT appears to project to the lateral subnuclei but I have not ascertained whether it synapses there.

Cajal (1952) has described the endings of this fiber tract as showing extensive ramification throughout the nucleus so that such a conclusion might be premature until appropriate silver stains can be done. Massopust and Thompson (1962) have described efferent fibers in the HPT which terminate in the dorsolateral and dorsomedial thalamic nuclei and the lateral habenular nucleus, some traveling with the stria medullaris to terminate in the anterior hypothalamus. The existence of this pathway might explain why Smaha (1968) observed a rostrally projecting efferent fiber bundle arising from IPN.

#### Comparative Studies

In order to place the rat into the schema of the total order Rodentia, comparative studies have been conducted on several members of the suborders Caviomorpha and Sciuromorpha (paper in preparation). The rat has been taken to be the sole representative of the Myomorpha. Quantitative measurements of the cell size and packing density within the IPN subnuclei have been conducted on the guinea pig, Cavia, and the capybara, Hydrochoerus, two representatives of the Caviomorpha. Quantitative studies of the nuclear configuration of representatives of the Sciuromorpha have been conducted on the mountain beaver, Aplodontia. Qualitative studies have been conducted on the chinchilla, Chinchilla, a caviamorph, and the gray squirrel, Sciurus, the marmot, Marmota, the flying squirrel, Glaucomys, and the eastern pocket gopher, Geomys, which are members of Sciuromorpha.

Generally the IPN of all of the above mentioned rodents can be divided into the four subnuclei described for the rat with one exception. In the capybara, a discrete pars lateralis does not appear to exist. Rather, the large celled dorsal division appears to extend ventrally around the lateral extent of the nucleus. The small celled dorsal subnucleus has the same configuration in the other rodents studied as seen in the rat. In the rostral extent of its course it moves ventrally to occupy the whole extent of the nucleus in planes of section through the red nucleus. Pars medialis has essentially the same relative extent and position throughout all of the rodents studied.

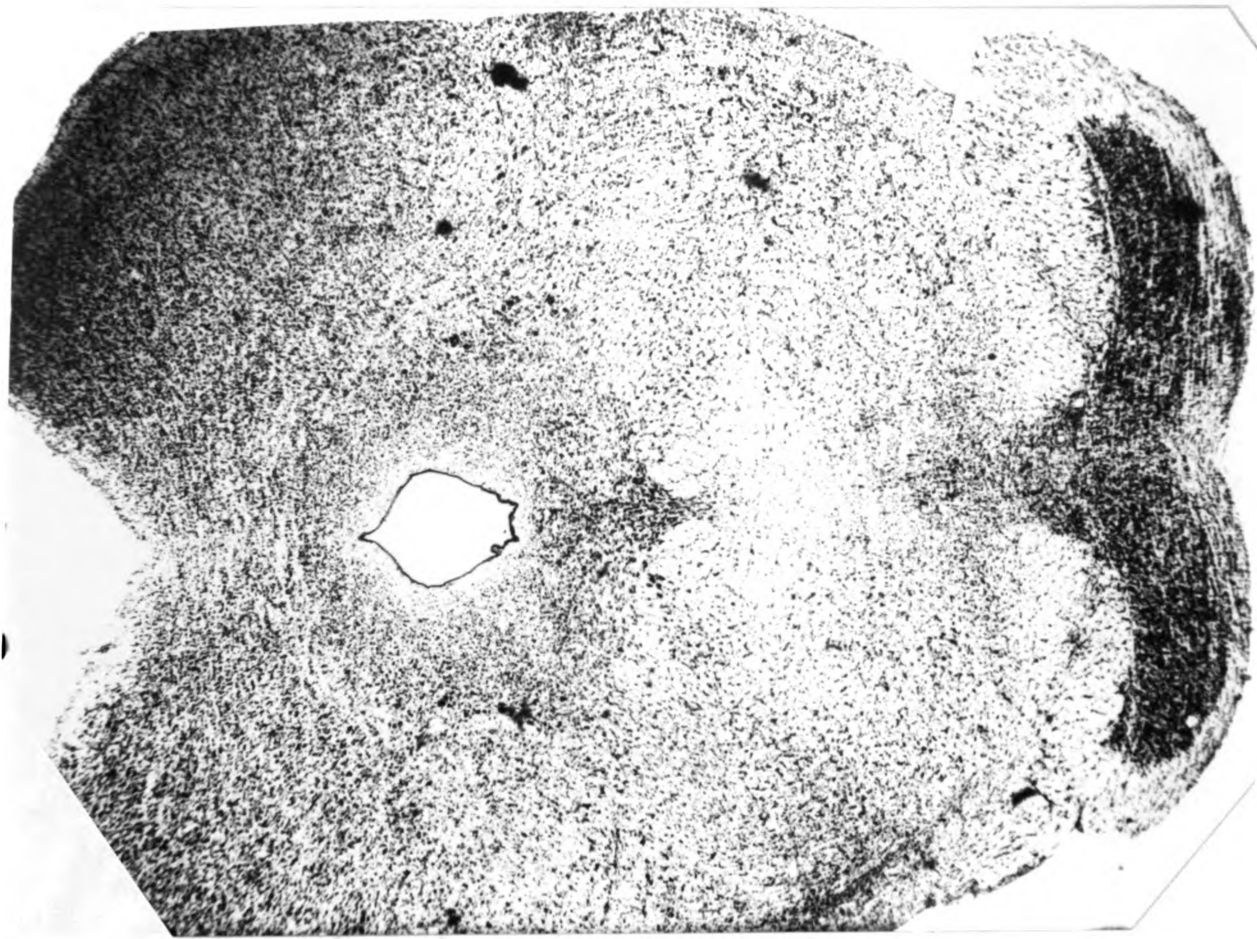
An important qualitative observation concerns the relation between the large celled dorsal division and the nucleus centralis superior, a nucleus of the median raphe. In all of the rodents mentioned above it has been noted that this large celled division is intimately related to the nucleus centralis superior. Furthermore, the size of PDM seems to be correlated with the size of this latter nucleus. In rodents such as the guinea pig, where the nucleus centralis superior is small, PDM was found to be correspondingly reduced in size. In the mountain beaver, where nucleus centralis superior is large, PDM was correspondingly well developed.

## REFERENCES

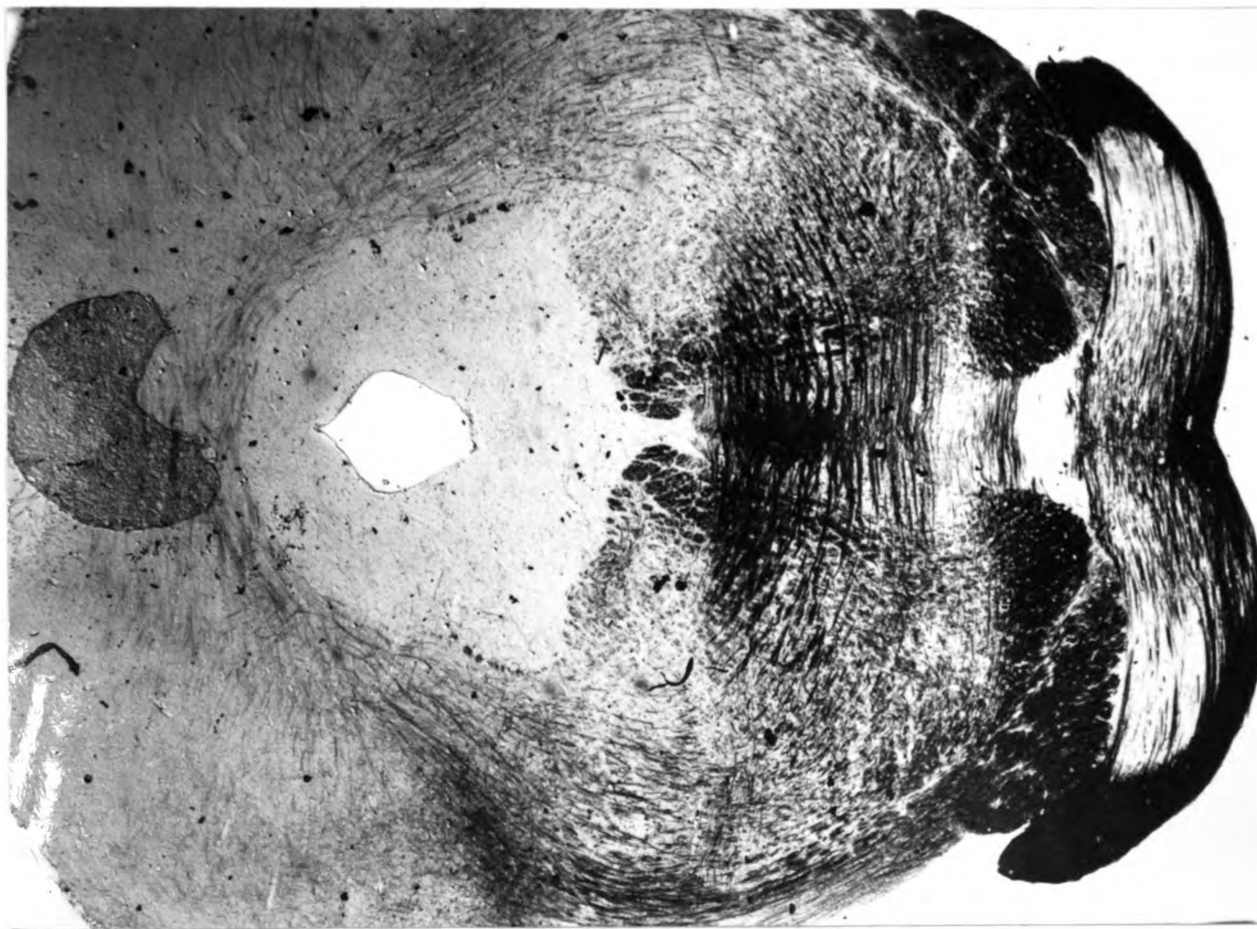
- Berman, A. L. and Bowers, S. R. A cytoarchitectonic analysis of the interpeduncular complex of the cat. Anat. Rec., 1967, 157, 213. (Abstract)
- Forel, August. Untersuchen die Haubenregion und ihre oberen Verknuepfungen im Gehirne des Menschen und einiger Saegethiere mit betraegen Zuden Methoden der Gehirnuntersuchung. Archiv. Psychiat. und Nervenkrankheiten, 1877, 7, 393-495.
- Friede, R. L. Histochemical investigations on succinic dehydrogenase in the central nervous system. III. Atlas of the midbrain of the guinea pig, including pons and cerebellum. J. Neurochem., 1959, 4, 290-303.
- Gudden, B. Mittheilung ueber das Ganglion interpedunculare. Archiv. Psychiat. und Nervenkrankheiten, 1881, 11, 424-427.
- Herrick, C. J. The internal structure of the midbrain and thalamus of Necturus. J. Comp. Neurol., 1917, 28, 215-348.
- Huber, G. C., Crosby, E. C., Woodburne, R. T., Gillian, L. A., Brown, J. O., and Tamthal, B. The mammalian midbrain and isthmus regions. Part I. The nuclear pattern. J. Comp. Neurol., 1943, 78, 129-536.
- Jansen, Jan. The brain of Myxine glutinosa. J. Comp. Neurol., 1930, 49, 359-507.
- Kappers, C.U.A., Huber, G. C., and Crosby, E. C. The Comparative Anatomy of the Nervous System of Vertebrates Including Man. New York: Macmillan, 1936, reprinted by Hafner, New York, 1960.
- Manocha, S. L. and Bourne, G. H. Histochemical mapping of succinic dehydrogenase and cytochrome oxidase in the pons and mesencephalon of squirrel monkey (Saimiri sciureus). Exp. Brain Res., 1966, 2, 230-246.
- Massopust, L. C. and Thompson, R. A new interpedunculo-diencephalic pathway in rats and cats. J. Comp. Neurol., 1962, 118, 97-106.
- Ramon y Cajal, S. Histologie du systeme nerveux de l'Homme et des Vertebres. Madrid: Consejo Superior de Investigaciones Cientificas, Instituto Ramon y Cajal, 1952.
- Sharrer, E. Capillaries and mitochondria in the neuropil. J. Comp. Neurol., 1945, 83, 237-243.

Smaha, L. A. Efferent fiber connections of the interpeduncular nucleus of the cat. Anat. Rec., 1968, 160, 430.  
(Abstract)

Zeman, W. and Innes, J. R. M. Craigie's Neuroanatomy of the Rat. New York: Academic Press, 1963.



Thionin



Haldenhain

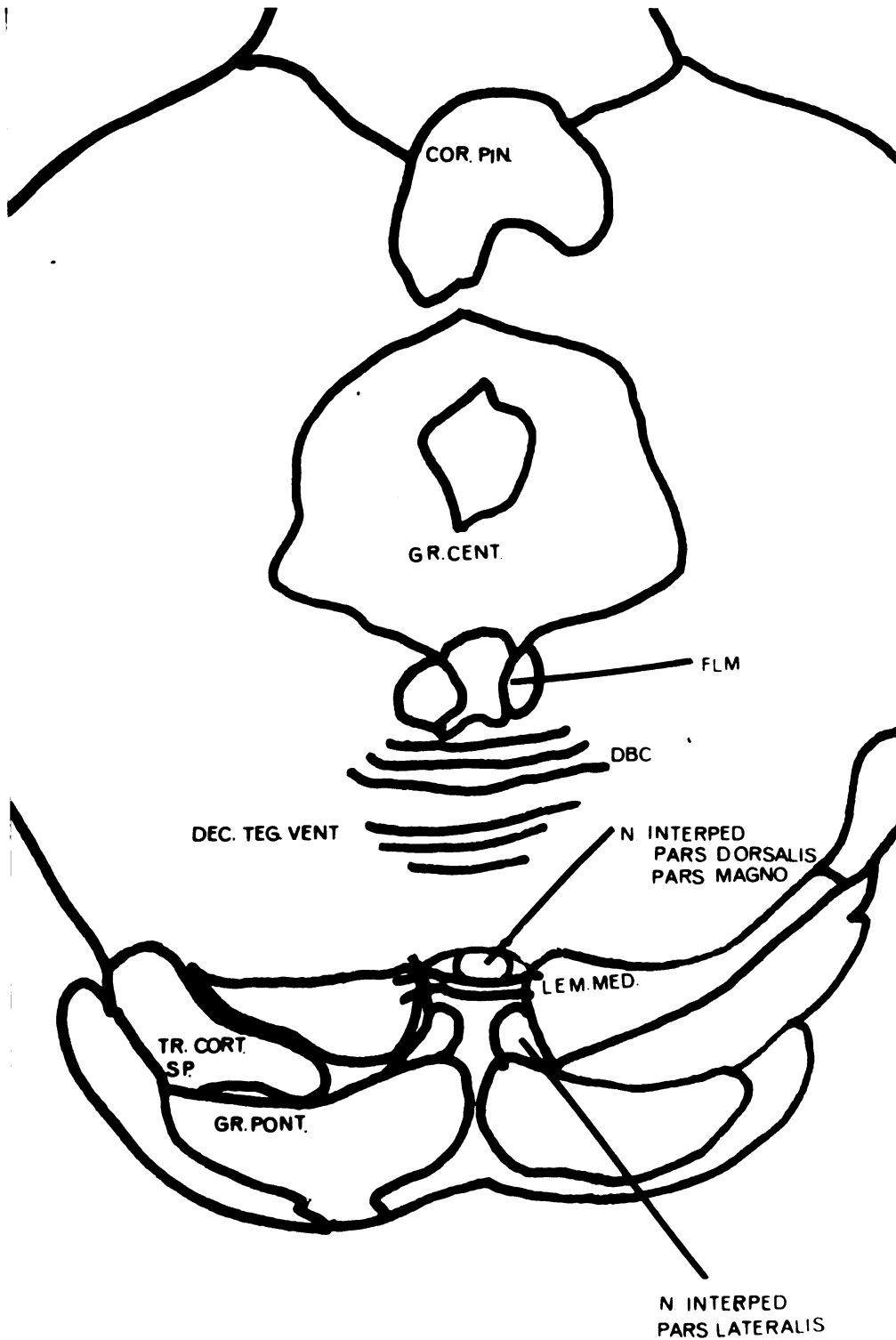
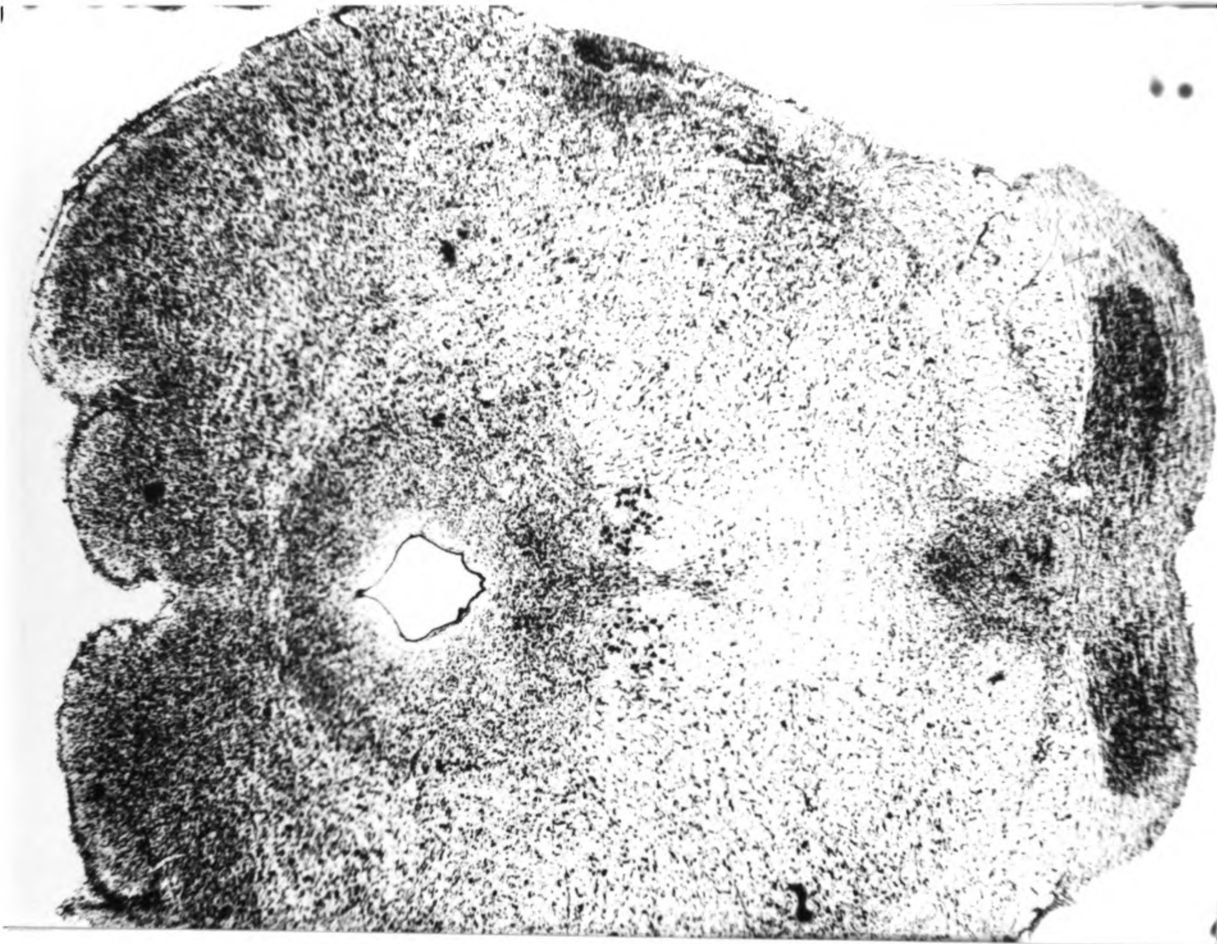
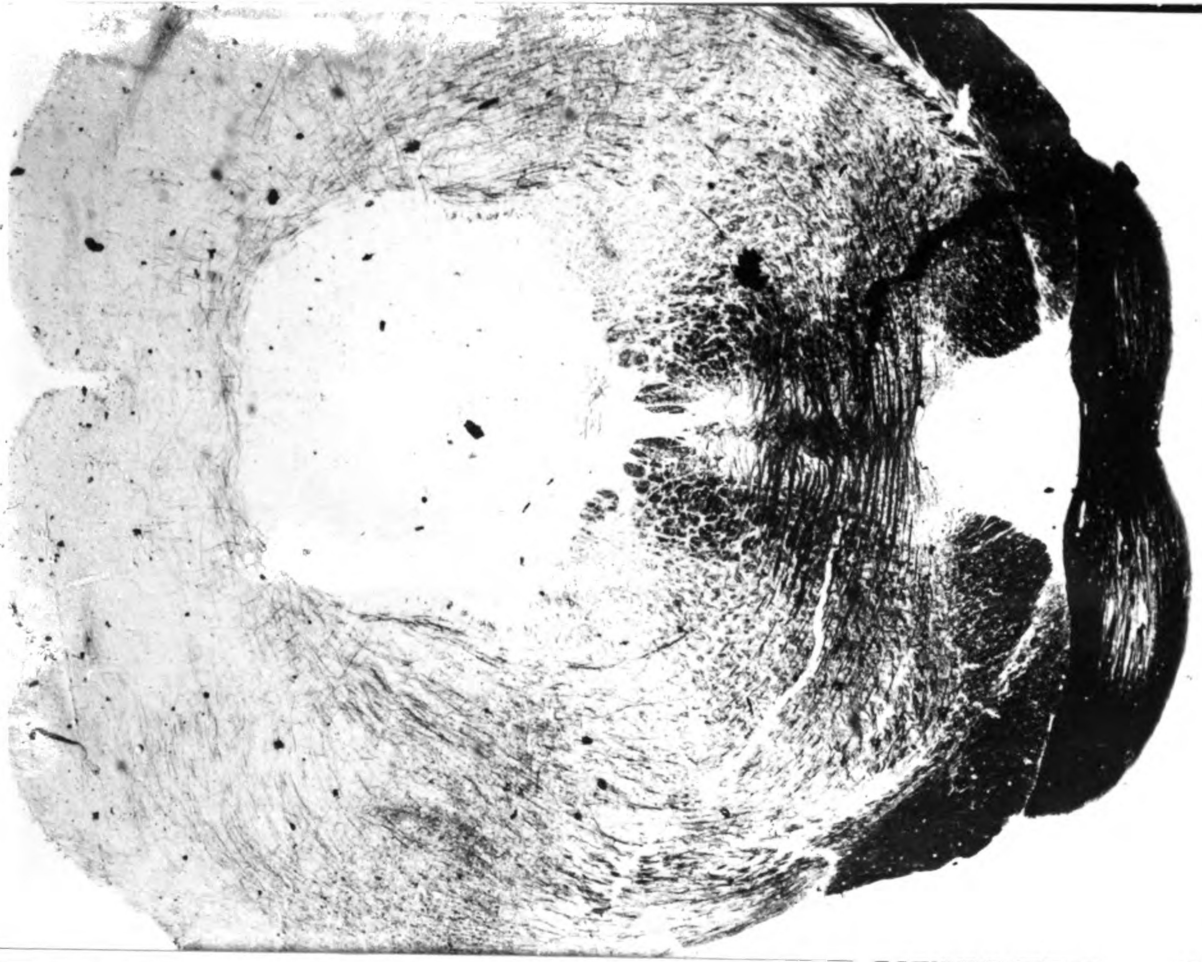


Plate 1. Caudal section through the midbrain at the level of the decussation of the superior cerebellar peduncle (DBC). In this and the following plates the midbrain is magnified 30 times. For a further description refer to the text.



Thionin



Haidenhain



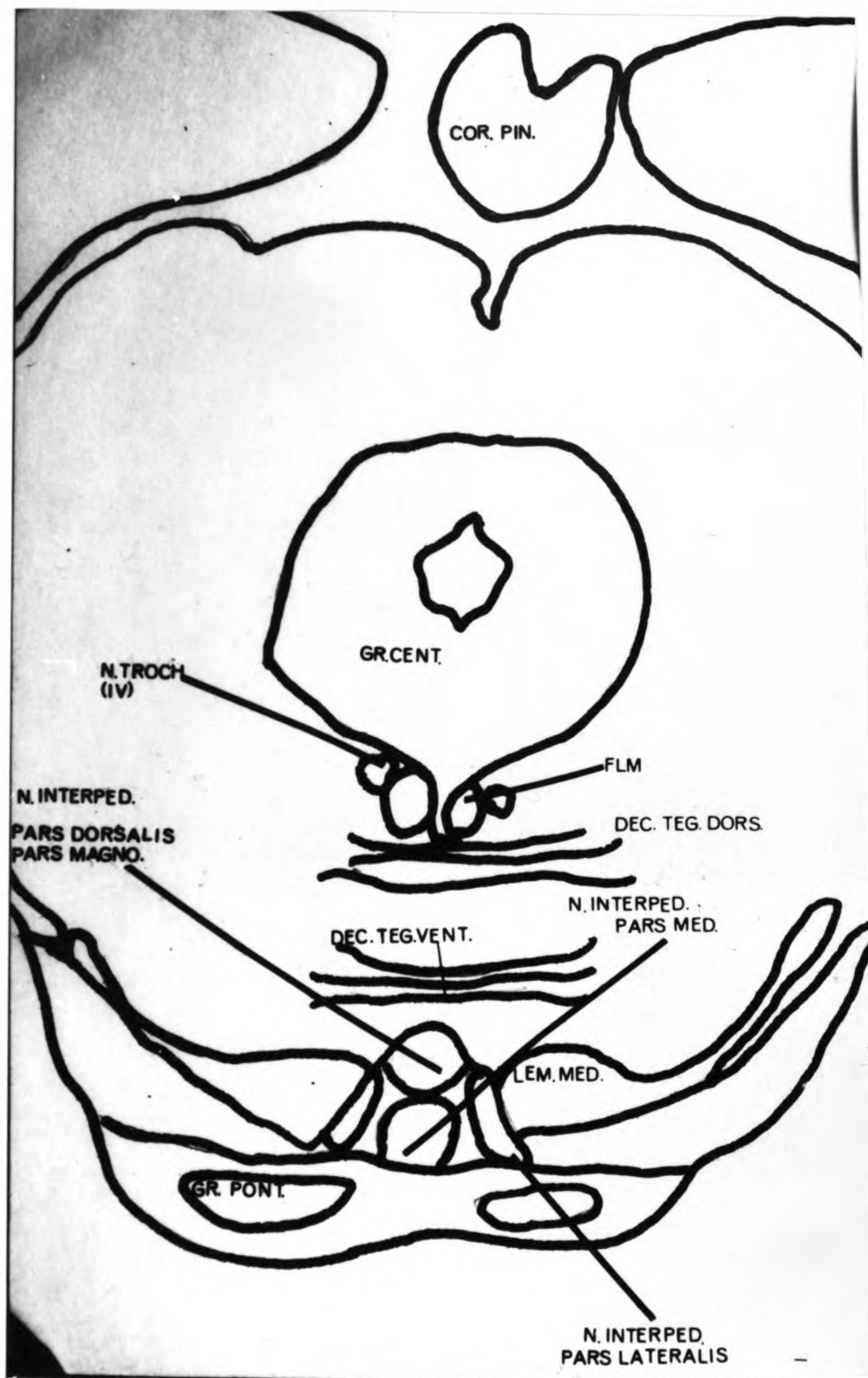
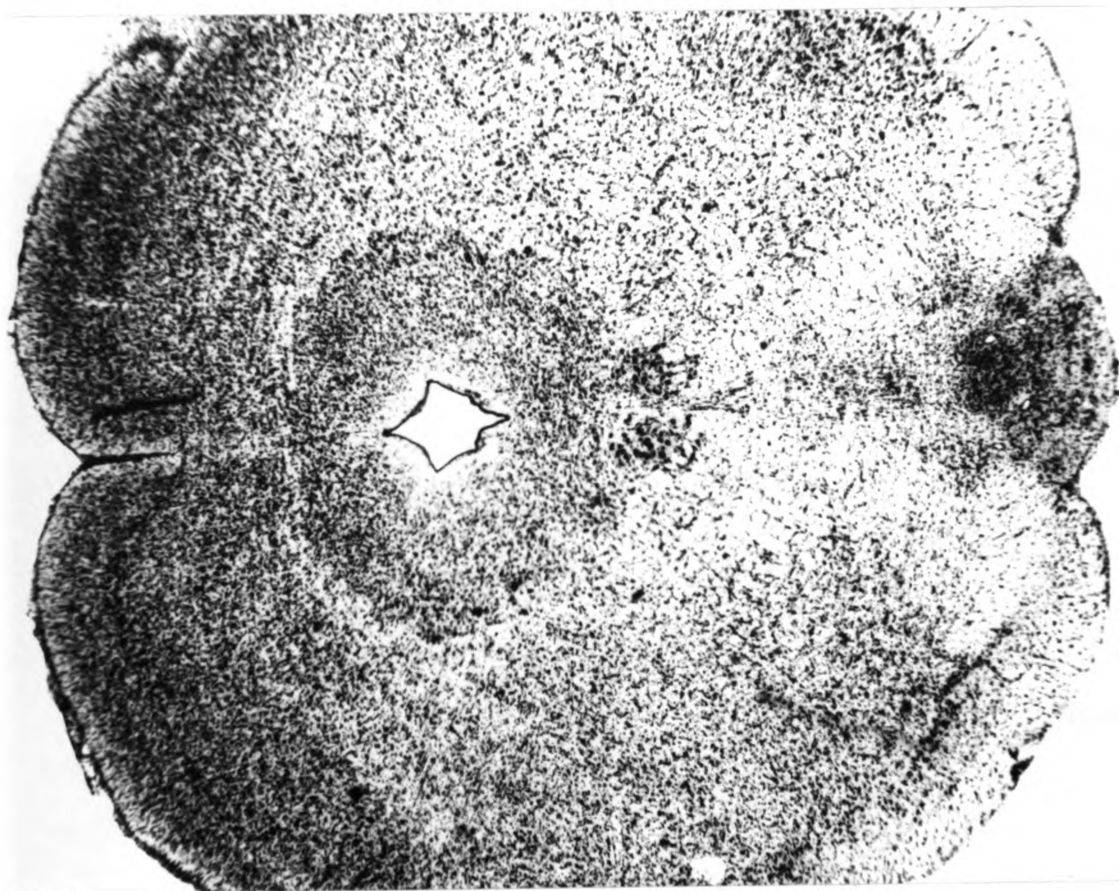
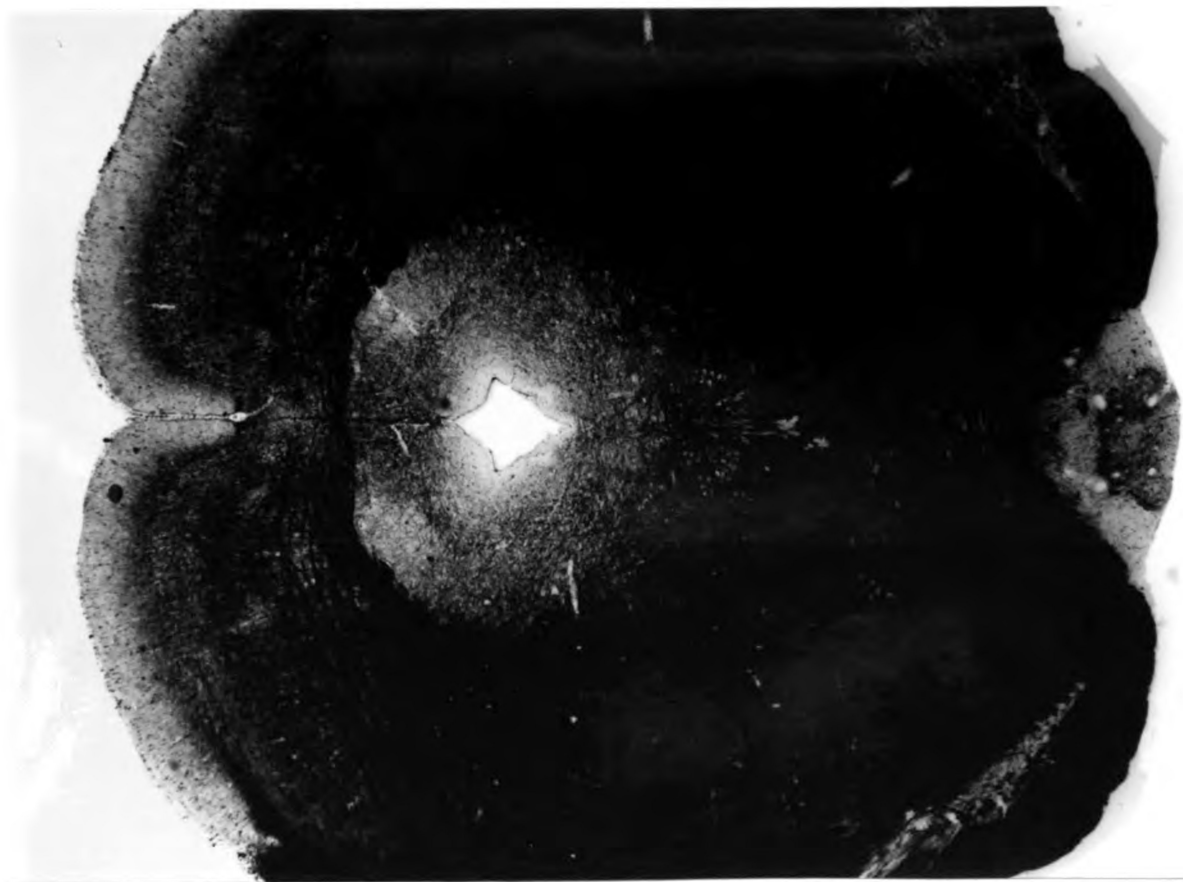


Plate 2. Caudal section through the midbrain at the level of the trochlear nucleus (IV). For a description of the IPN at this level refer to the text.



Thionin



Haidenhain

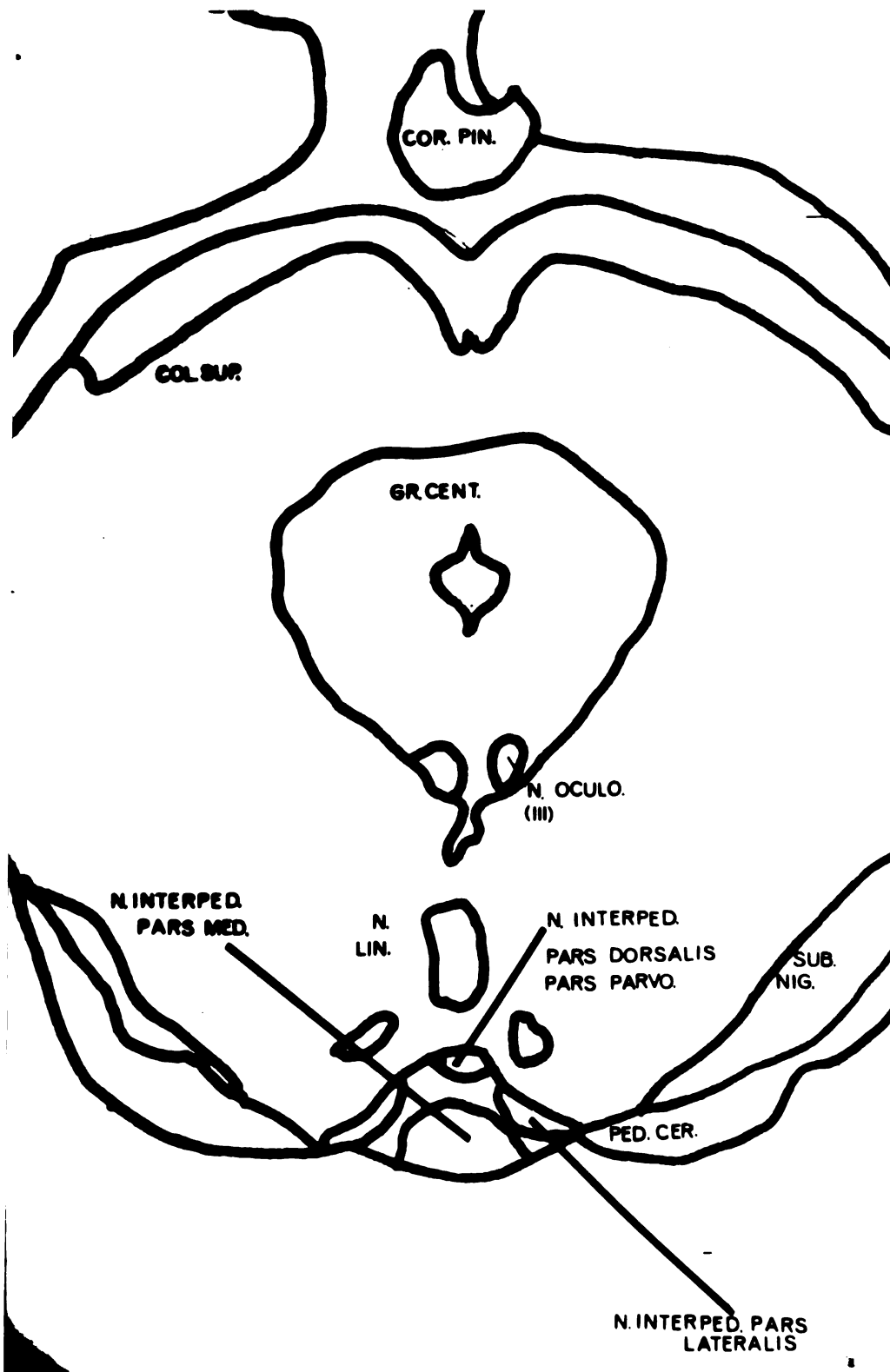
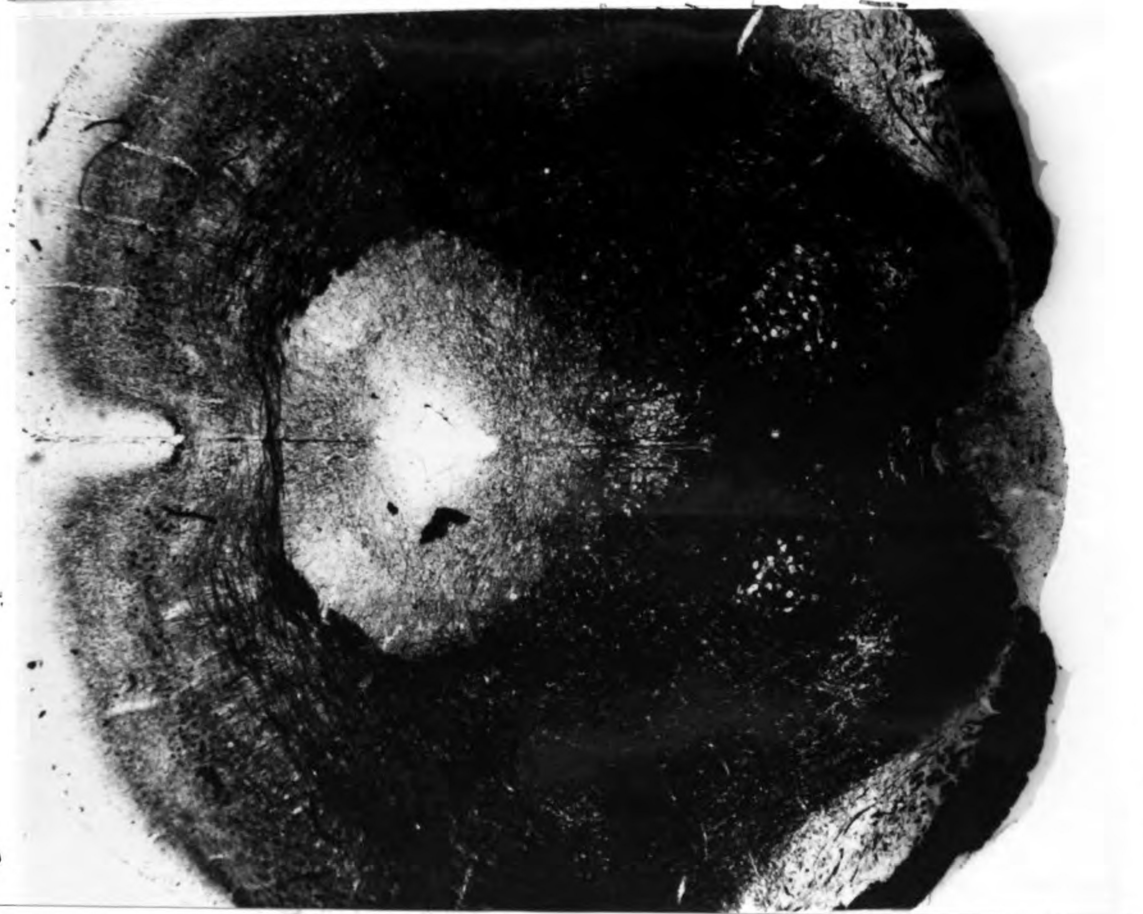
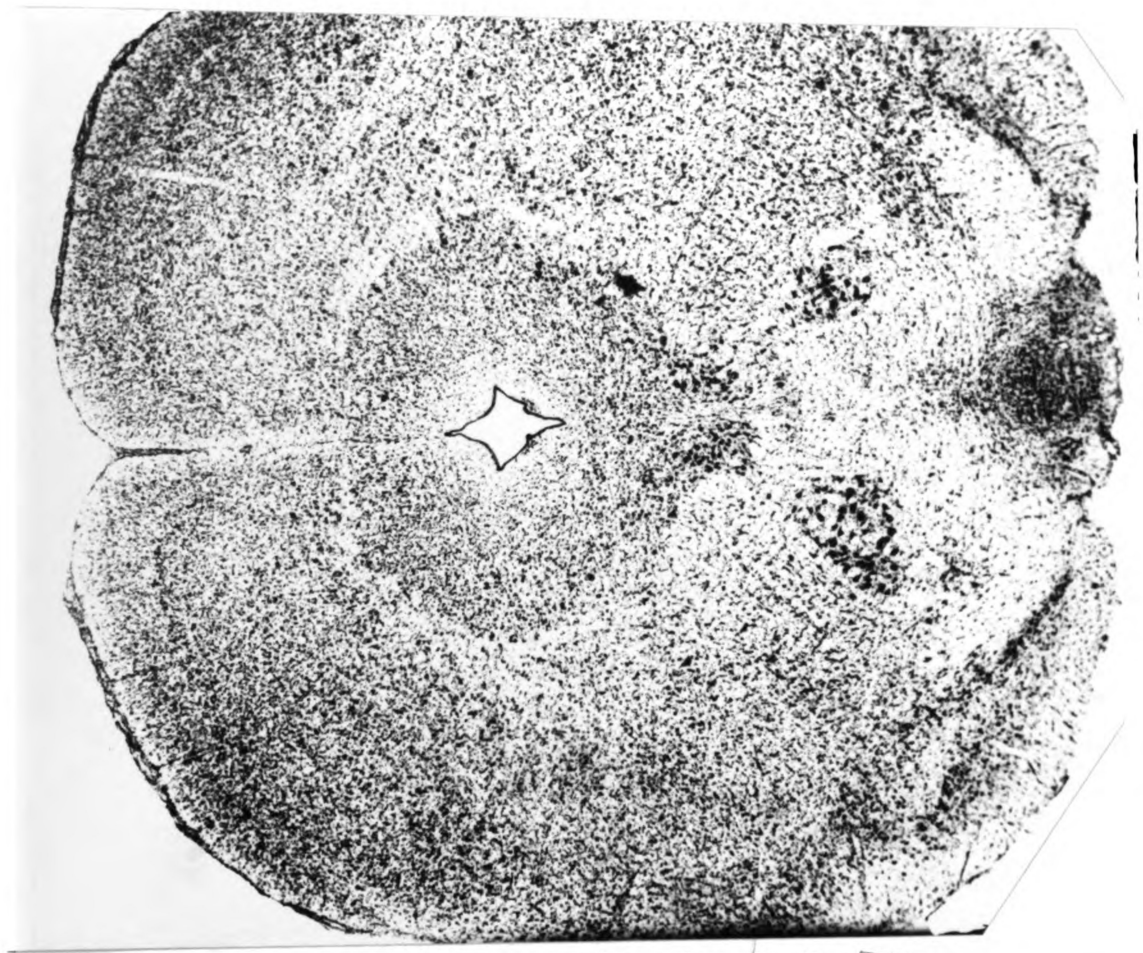


Plate 3. Coronal section through the midbrain at the level of the caudal extent of the superior colliculus (COL. SUP.). For a description of the IPN at this level refer to the text.



Haidenhain



Thionin

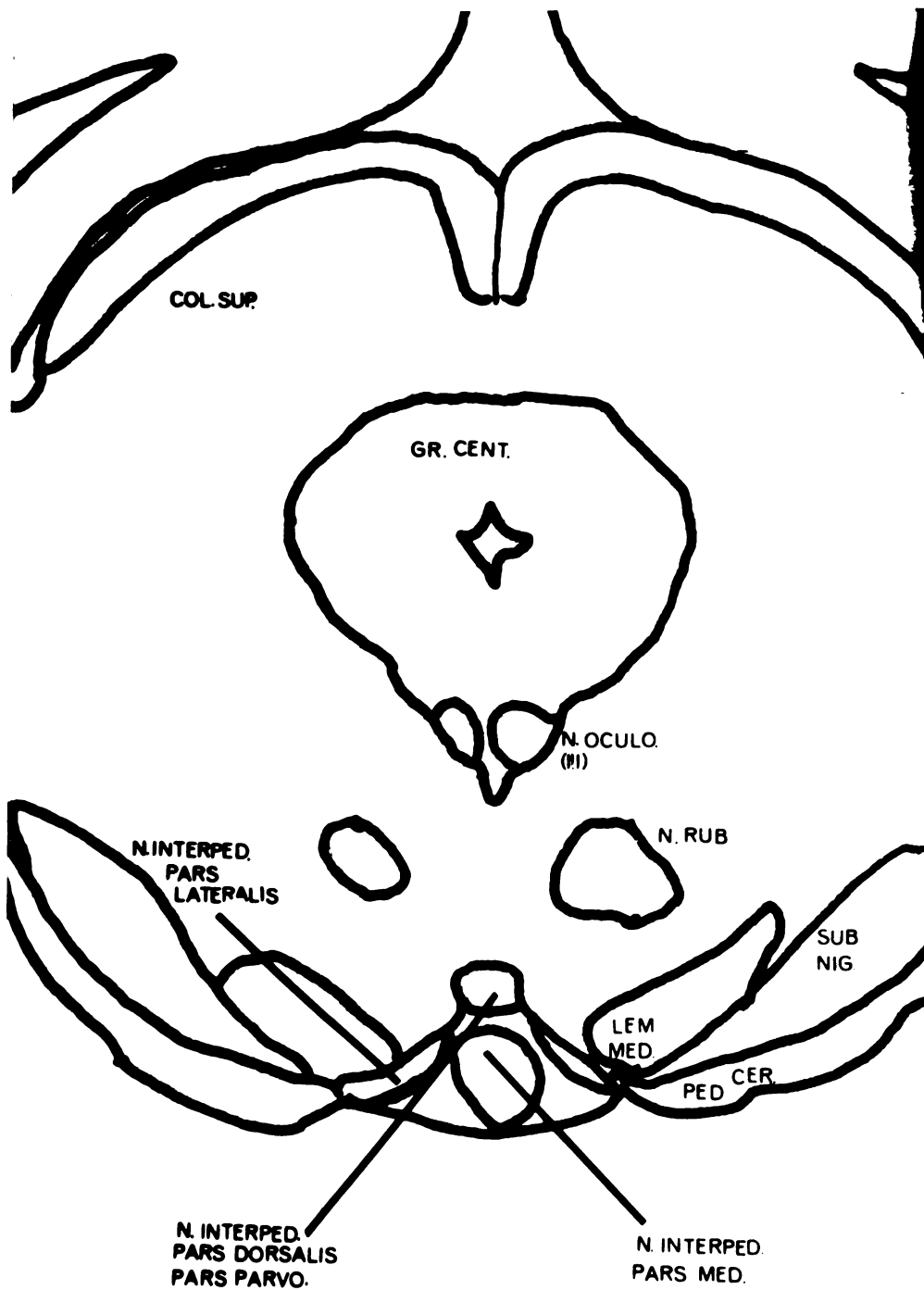
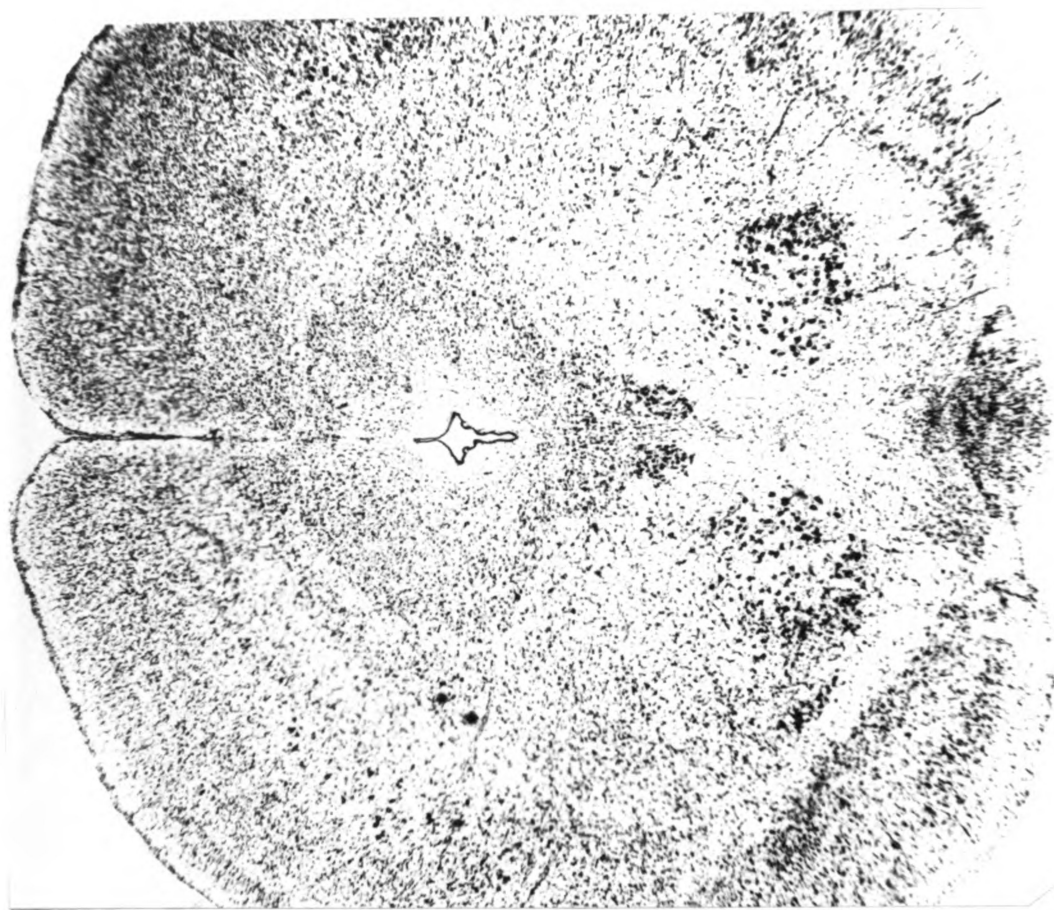
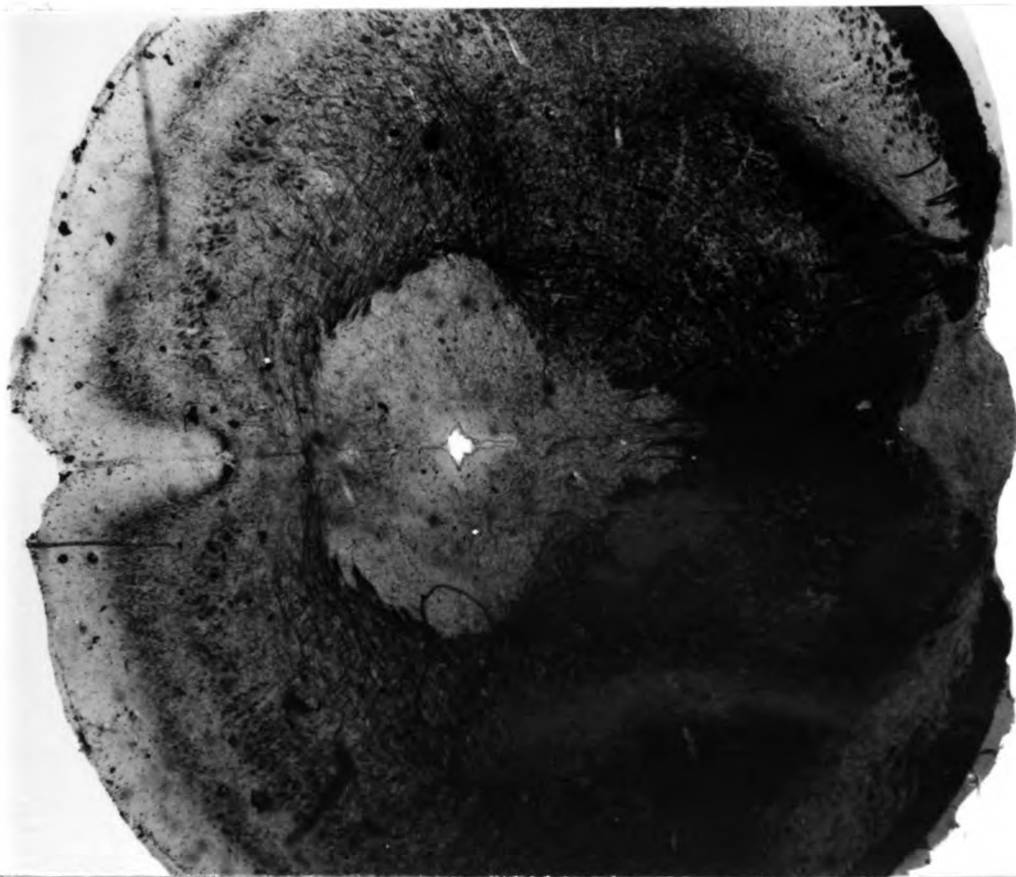


Plate 4. Coronal section through the midbrain at the level of the oculomotor nucleus (III). For a description of the IPN at this level refer to the text.



Thionin



Haidenhain



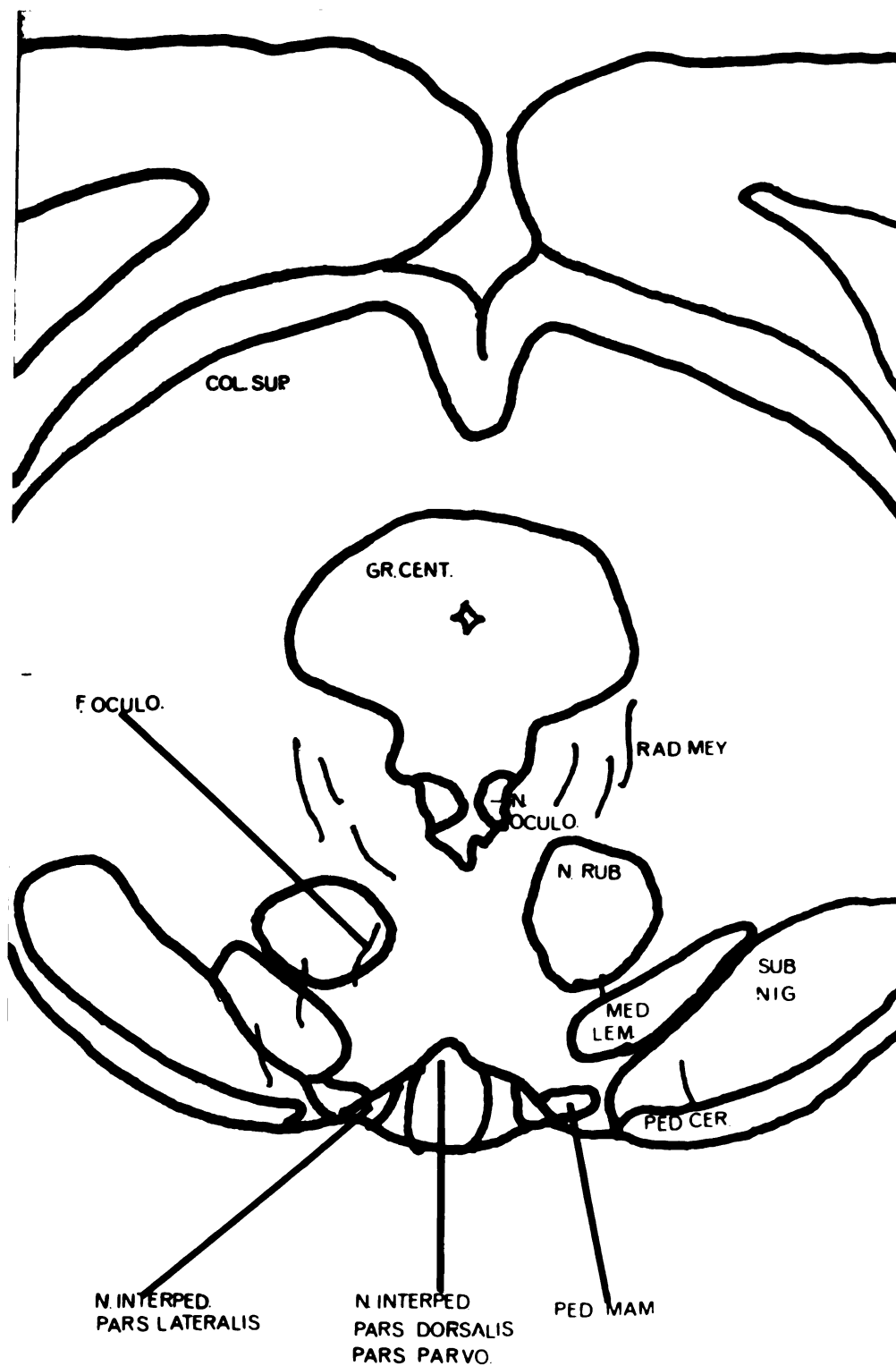
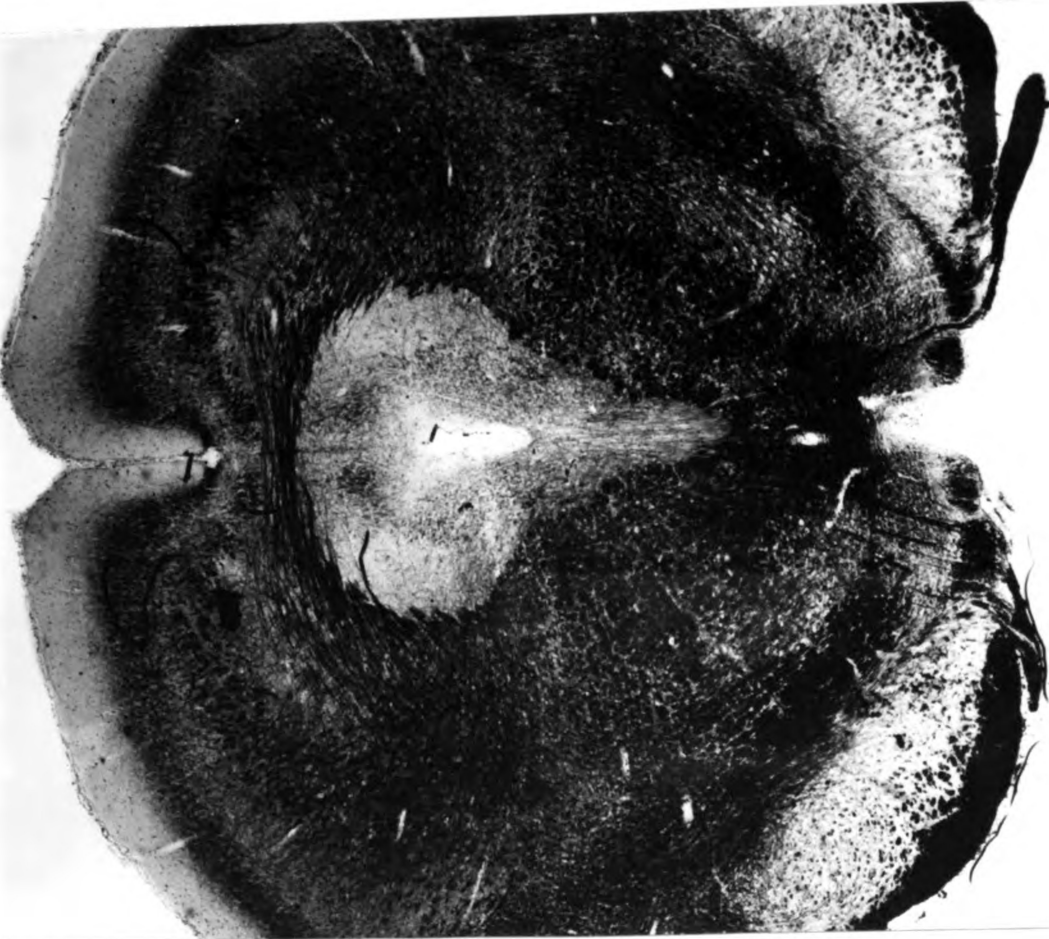


Plate 5. Coronal section through the midbrain at the level of the red nucleus (N. RUB.). For a description of the IPN at this level refer to the text.



Thionin



Haidenhain



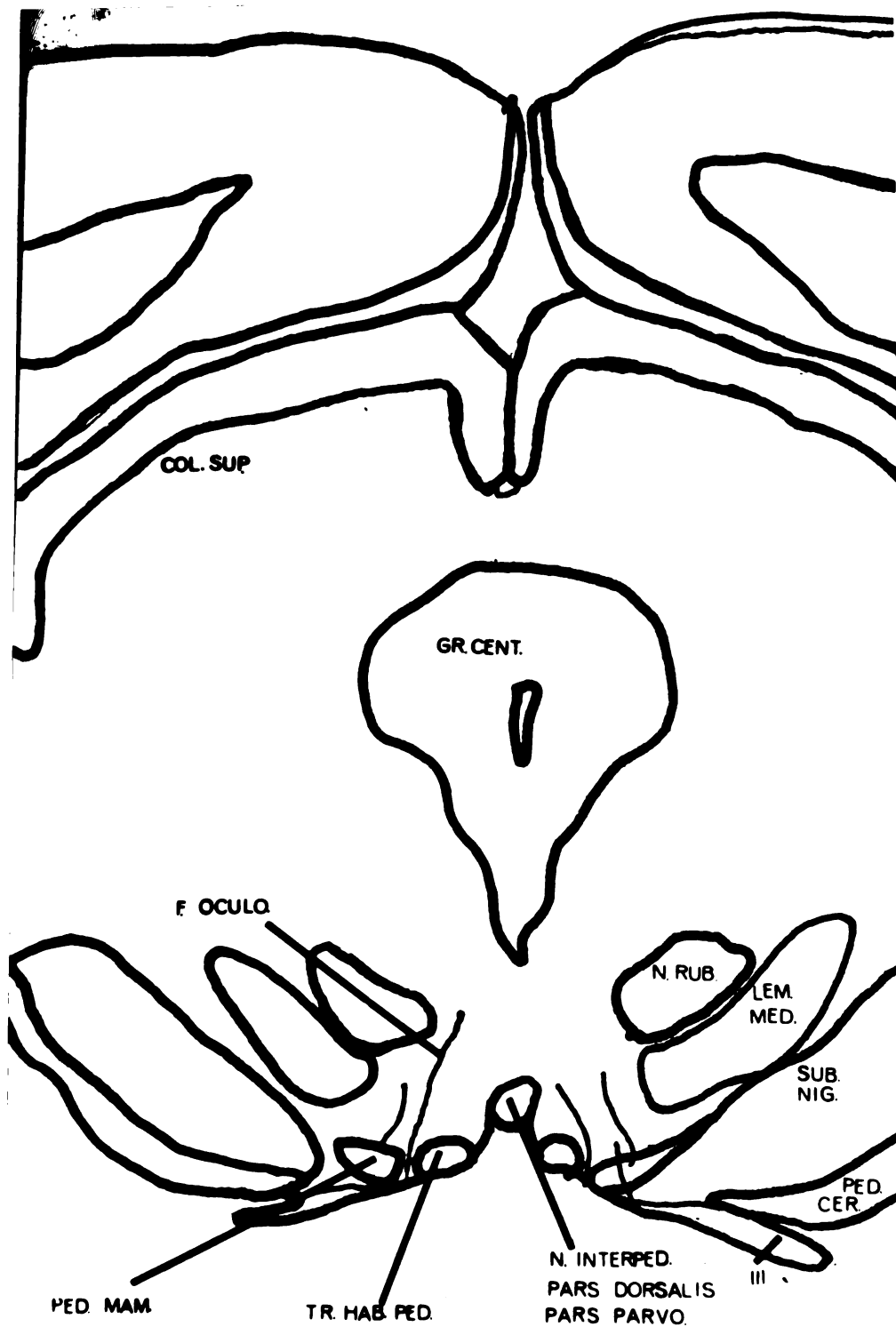


Plate 6. Coronal section through the midbrain at the rostral end of the IPN. For a description of the nucleus at this level refer to the text.

## APPENDIX A

### THIONIN STAIN (NISSL METHOD)

1. Take sections off paper by floating each section into distilled water.
2. From the distilled water place the sections in the steaming stain (buffered to pH 4.0) in the oven for 15 min. (1% thionin sol.)
3. Transfer the sections to distilled water.
4. Transfer the sections to 80% ethyl alcohol and agitate to remove excess stain.
5. Place sections in aniline alcohol (50 cc. aniline, 450 cc. 95% ethyl alcohol). Change to fresh aniline as the color comes out.
6. When the sections are the desired color transfer to 95% alcohol and wash through 6 changes of 95% to remove the aniline
7. Clear sections in oil of cajeput rinse in at least 2 changes of xylene and mount in H.S.R. mounting medium or Permount.

\*\*\*\*\*

### SANIDES HAIDENHAIN MYELIN STAIN

- Solutions:
1. 2.5% ferric ammonium sulfate
  2. 10% hematoxylin in absolute ethyl alcohol allowed to sit for 2 weeks in the sunlight unstoppered.
  3. Saturated lithium carbonate (store in refrigerator)
1. Place sections in distilled water for 1 hr. and change to fresh distilled water for a second hour.
  2. Place 15-20 small sections or 5-7 large sections in a petri dish of solution 1 and allow to stand overnight.
  3. Prepare staining solution of 50 cc. distilled water, 5 cc. solution 2, and 3-7 ml. of solution 3.
  4. Pour the ferric ammonium sulfate solution off the sections and rinse in 2 changes of distilled water.
  5. Pour the staining solution over the sections and let stand for 5 hours being sure to agitate the sections every hour.
  6. Pour off stain, rinse in 3 changes of distilled water, and let sections stand in 80% alcohol until clear of reddish color.

## APPENDIX A

### SANIDES HAIDENHAIN MYELIN STAIN (continued)

7. Pour on fresh 80% alcohol and let stand overnight.
8. Place sections in 95% alcohol for at least 24 hrs.
9. Dehydrate sections in one change of 95% alcohol and one change of absolute alcohol.
10. Drain and put through 2 changes on xylene and mount as described for the thionin stain.

MICHIGAN STATE UNIV. LIBRARIES



31293100709785